UNIVERSITY OF CALIFORNIA,
IRVINE

Bubble Nucleation and the Electroweak Phase Transition

DISSERTATION

submitted in partial satisfaction of the requirements
for the degree of

DOCTOR OF PHILOSOPHY

in Physics

by

Arianna Braconi

Dissertation Committee:
Professor Mu-Chun Chen, Chair
Professor Timothy Tait
Professor Yuri Shirman

2021

DEDICATION

Dedicated to my parents and Korrigan Clark.

TABLE OF CONTENTS

LIST OF FIGURES

ACKNOWLEDGMENTS

I am extremely grateful to the wide community of people who have supported me throughout this endeavor. I am especially grateful to my advisor, Mu-Chun Chen, whose support and mentorship guided me through this process, as well as the whole physics community at UC Irvine for providing me with a welcoming and supportive environment in which to study physics.

The work presented in this dissertation is in part supported by Department of Education GAANN Grant No. P200A150121at UC Irvine.

I also must thank my office mates, who made our windowless grad office a fun and productive work environment. I am especially grateful to Alexis Romero, Freida Rivera, Michael Waterbury, Ben Lillard, Sunny Yu, and Jordan Smolinsky. I also owe a deep debt of gratitude to my friends who were not confined to an office with me, but chose to put up with me voluntarily during this time. For this I thank Agnes Eshak, Miriam Botros and Cindy Huynh.

And finally I must thank my family who have provided me with a lifetime of love and support.

VITA

Arianna Braconi

EDUCATION

Doctor of Philosophy in Physics — **2021**
University of California, Irvine — *Irvine, CA*

Master of Science in Physics — **2015**
City College of New York — *New York, New York*

Bachelor of Art — **2012**
Queens College — *Flushing, New York*

RESEARCH EXPERIENCE

Graduate Student Researcher — **2016–2020**
University of California, Irvine — *Irvine, California*

TEACHING EXPERIENCE

Lecturer — **2019, 2020**
University of California, Irvine — *Irvine, CA*

Teaching Assistant — **2016–2020**
University of California, Irvine — *Irvine, CA*

Adjunct Lecturer — **2015–2016**
City College of New York — *New York, NY*

AWARDS AND FELLOWSHIPS

Dissertation Fellowship — **2020**
Department of Physics and Astronomy, University of California, Irvine

Chancellor's Fellowship — **2016–2018**
Department of Physics and Astronomy, University of California, Irvine

SERVICE AND LEADERSHIP

Women in Physics and Astronomy — **2016–2020**
University of California, Irvine

Teaching Assistant Advocate — **2019–2020**
Physics Graduate Caucus, University of California, Irvine

ABSTRACT OF THE DISSERTATION

Bubble Nucleation and the Electroweak Phase Transition

By

Arianna Braconi

Doctor of Philosophy in Physics

University of California, Irvine, 2021

Professor Mu-Chun Chen, Chair

While the Standard Model of particle physics has been extremely successful in describing particle interactions, there are still phenomena that remain unexplained. The asymmetry between matter and antimatter in our universe is one of the most obvious unanswered questions, and the lack of a fundamental understanding of the origin of the parameters in the flavor sector is another important unanswered question.

It might be possible for a mechanism to address both of the above issues. If the electroweak phase transition was first order, it could be possible to create the observed matter-antimatter asymmetry during this time. Additionally, it has been proposed that large Yukawa couplings could generate the necessary CP-violation to produce the observed baryon asymmetry that the Standard Model currently lacks.

This may be implemented via the Froggatt-Nielsen mechanism, which would have the additional benefit of addressing the problem in the flavor sector as well. It has been proposed that implementing the Froggatt-Nielsen mechanism to produce large Yukawa couplings that vary during the electroweak phase transition could produce a strong enough phase transition needed for successful electroweak baryogenesis.

First order phase transitions proceed via the nucleation of bubbles, which percolate and

expand, eventually filling the entire universe with the new phase. Calculating the bubble nucleation rate is not always simple, and it has been pointed out that in some models with an additional scalar, bubbles actually fail to nucleate. This means that where a first-order phase transition is naively expected, there is actually no phase transition at all.

The study of bubble nucleation in the case of large Yukawa couplings that vary during the electroweak phase transition will be undertaken here, and we will see that the potential barrier height plays an important role in the nucleation of bubbles.

Chapter 1

Introduction

There are still many physical phenomena that our current Standard Model of particle physics cannot explain, and these unexplained phenomena hint at new physics beyond the Standard Model.

One of the most obvious unexplained phenomena is the huge asymmetry in our present universe between matter and antimatter. Our universe seems to be made up of only matter, and no antimatter. It is unlikely that our universe began with such a mismatch between baryons and antibaryons, so it is reasonable to instead search for processes in the early universe that could produce such an asymmetry.

Another unexplained mystery is what is called the "Flavor Problem." For some reason, our universe produces three generations of matter, each more massive than the last. There is no apparent reason for this redundancy. Additionally, heavier quarks can decay into lighter quarks, and these mixing angles also exhibit a clear hierarchy. Such a clear hierarchy would suggest some deeper structure to the masses and mixing angles in the quark sector. It is also unclear why the masses span such a huge range of magnitudes; the lightest quark, the up quark, is only 2 MeV, while the heaviest quark, the top quark, is 173 GeV, a difference

of nearly six orders of magnitude.

It is interesting to consider scenarios where these two problems have a common solution. The most obvious path is to consider that perhaps the matter-antimatter asymmetry was produced during the electroweak phase transition, the time when the electromagnetic and weak forces separated from a single unified force into the two distinct forces we observe today. This is an attractive possibility because the electroweak scale is around 100 GeV, which is accessible to current experiments, so it is a theory that is currently testable.

As mentioned above, in our present universe, electroweak symmetry is broken, but in the early universe, within a nanosecond of the Big Bang, when temperatures were much hotter, this symmetry was unbroken. A matter-antimattery asymmetry can be generated during a phase transition from unbroken to broken symmetry, if the phase transition meets certain criteria and there is sufficient CP-violation. In the Standard Model, the electroweak phase transition is what is known as a "crossover," and there is not a sufficient source of CP-violation to explain the observed abundance of baryons over antibaryons, so we must search elsewhere.

If the electroweak phase transition can be shown to have been first order, which proceeds via nucleation of bubbles, it could possibly explain the matter-antimatter asymmetry in our universe [1]. Any mechanism which produces a baryon-antibaryon asymmetry during the electroweak phase transition is called Electroweak Baryogenesis [2].

In order for the electroweak phase transition to be strongly first order, it requires physics beyond the Standard Model. The simplest extension to the Standard Model which can produce a first order phase transition is the addition of a singlet scalar [3, 4, 5] that couples to the Higgs via interactions of the form $V_{\text{int}} = \kappa H^2 S^2$ where H is the Higgs and S is the new scalar.

It is known that the Standard Model does not produce sufficient CP-violation to create

the observed baryon asymmetry [6, 7], this is due to the parameters in the CKM matrix being too small. It was proposed in [8] that if the value of the Yukawa couplings was large (order one) at the time of the electroweak phase transition, that this could possibly produce sufficient baryon asymmetry to match observation. It was also shown in [9] that a first order phase transition may be possible if the Yukawa couplings were order one before the phase transition, and actually varied throughout the phase transition. This can be implemented via the Froggatt-Nielsen mechanism which is connected to the flavor problem, potentially addressing both the mattery-antimatter asymmetry problem and the flavor problem. We will be exploring this possibility further.

Studies of phase transitions are typically computationally very intense, so oftentimes simple approximations are used. However, some of these approximations may miss important aspects of the phase transition. In [10], the dynamics of bubble nucleation during the electroweak phase transition in the presence of an extra scalar was explored. It was found that for most of the parameter space where a first order phase transition was naively expected, bubbles fail to nucleate at any temperature. This means that the phase transition cannot proceed and thus cannot be first order. This has important implications in that it drastically limits the allowed parameter space for electroweak baryogenesis that was previously considered acceptable.

In the present analysis, the dynamics of bubble nucleation were studied in scenarios with large and varying Yukawas coupling constants, and it was found that bubbles do not nucleate in many of the scenarios studied, and bubble nucleation only occurred in a narrow range of parameters.

1.1 A Brief History of the Early Universe

The expansion of the universe implies that it was denser and hotter in the distant past, originating in a "Big Bang." In order to better understand early universe phase transitions, it is helpful to be familiar with the evolution of the early universe.

It is theorized that immediately after the Big Bang, when temperatures were above 10^{16} GeV, all of the three fundamental forces described in the Standard Model were unified into a single Grand Unified Force. There are, of course, issues with this, and questions remain whether the universe even achieved temperatures this high immediately after the Big Bang since there is no direct evidence of temperatures above a few MeV.

At some point, as the universe began to expand and the temperature of the universe cooled, the three forces would have separated into the strong and electroweak forces via a phase transition.

As the universe cooled further, to temperatures around 100 GeV, the electroweak phase transition took place. This phase transition separated the electroweak force into the separate weak and electromagnetic forces that we know today. Prior to this phase transition, the Higgs was in its symmetric phase with background value $\langle\phi\rangle = 0$, and hence all particles were massless. After the phase transition, the particles assumed a mass as the Higgs assumed its nonzero background expectation value $\langle\phi\rangle \neq 0$ that we have today. In the Standard Model this phase transition is a crossover, meaning the system changes smoothly from one phase to the another.

At lower temperatures, around 200 MeV (the scale of strong interactions), and just a few microseconds after the Big Bang, the transition from the quark-gluon plasma to hadronic matter took place. At higher temperatures quarks and gluons behaved as free particles in the plasma, while at lower temperatures after the phase transition they are confined to colorless

bound states. This phase transition is also thought to be a smooth crossover.

As the universe cooled further, to temperatures about 1 MeV to 50 keV, which corresponds to about 1-300 seconds after the Big Bang, neutrons and protons were captured into nuclei. Prior to this time, neutrons and protons moved freely within the primordial plasma. The nucleons condensed into light atoms, mostly helium, deutrium, and lithium (heavier elements were not synthesized yet and were instead produced during the stellar evolution). This is the epoch of Big Bang Nucleosynthesis.

After Big Bang Nucleosynthesis, the matter in the universe was in the state of a gas of mostly hydrogen. However, the binding energy was insufficient to keep the electrons bound in the atoms, and matter was in a state of baryon-electron-photon plasma. As the temperature decreased, the the plasma began to form atoms. This era is called Recombination. Before this period photons were scattered by electrons in the plasma, making the plasma opaque. After Recombination, the gas was transparent to photons. This means that the cosmic microwave background that we see today comes from the recombination epoch (about 370,000 years after the Big Bang).

1.2 Problems in the Standard Model

Currently, the Standard Model is used to describe particle interactions between three of the four fundamental forces. The Standard Model is based on an $SU(3)_c \times SU(2)_L \times U(1)_Y$ gauge group governing particle interactions and consists of three generations of quarks, three generations of leptons, a Higgs Boson, as well as gauge bosons to mediate the strong, weak and electromagnetic forces. While the Standard Model has been immensely successful in describing particle interactions, there are some glaring issues that cannot be explained within the structure of the Standard Model.

The first, and most obvious, is that the Standard Model only addresses interactions between three of the four fundamental forces; it completely neglects gravity. Not only that, the Standard Model is inconsistent with general relativity, and one or both theories must be modified. Much effort has been spent trying to correct this issue, and so far we still do not have an acceptable solution.

Another problem is the strong CP problem. Why does QCD allow for CP-violation in the strong force, but no such violation has ever been found? It would appear that the strong force then does, in fact, conserve CP symmetry, but why? The most well-known proposed solution to this problem is the addition of pseudoscalar particle called the axion, proposed by Peccei and Quinn [11].

Yet another problem is that Standard Model cannot explain why neutrinos have masses. According to the Standard Model, neutrinos should be massless, but it was discovered [12] in 1998 that neutrinos actually oscillate between flavors, which is only possible if they have a nonzero mass [13].

Another problem is dark matter and dark energy. Dark matter is thought to make up 26% of our universe, yet we do not know what it is! The most favored explanation is that it is a yet-undiscovered particle that interacts weakly or not at all with the other three fundamental forces [14]. Dark energy makes up nearly 70% of the energy density of the universe, and could explain the apparent (and also unexplained) increase in the expansion of the universe.

The two final problems are what we will concern ourselves with in the current paper: the matter-antimatter asymmetry of the universe and the "flavor problem," as mentioned previously. The universe is made up of matter, and not of antimatter, although there is no apparent reason for this. There is no reason why matter should be favored over antimatter, and no apparent reason why the initial conditions of the universe would favor one type of matter over the other. The Standard Model cannot explain this asymmetry of our uni-

verse, which is one of the prime motivations for the search for physics beyond the Standard Model [15].

The flavor problem [16], as mentioned above, is twofold: there is an obvious hierarchy in the masses and mixing angles of the six quarks, with no apparent explanation; and these masses also span six orders of magnitude. What causes such huge differences in quark masses? There is currently no answer.

The possibility that there is a connection between matter-antimatter and flavor problems is one which we will explore here. This possibility is intriguing because not only would it kill two birds with one stone, but it would have interesting cosmological implications for the evolution of the universe as well.

1.2.1 The Flavor Problem

In the Standard Model, there are 19 parameters (if we neglect neutrino masses): the three gauge couplings, the Higgs quartic coupling, and the Higgs mass squared make the first five. The remaining 14 are all found in the flavor sector: six quark masses, three lepton masses, four quark mixing angles, and the strong CP angle. If we add the parameters for addressing the neutrino sector, we will then have 23 out of 28 parameters relating to the flavor sector in the Standard Model [17, 18].

The origin of these physical parameters is unknown and unexplained within the Standard Model. Why are there three generations of quarks and leptons each with increasing mass? The strong hierarchical pattern of flavor parameters clearly does not seem arbitrary, are they connected in some way? The fermion masses exhibit a strong hierarchy, and the quark masses span six orders of magnitude. The mixing angles within the quark sector also exhibit a strong

hierarchy and are as of yet unexplained. The lack of understanding of such fundamental issues is called the "flavor problem." Since questions are not addressed within the Standard Model, all of these parameters must be input by hand.

The masses and mixing angles in the quark sector in the Standard Model arise from the Yukawa interactions, described by the lagrangian

$$\mathcal{L}_Y = -Y^d_{ij}\bar{Q}_{Li}\Phi D_{Rj} - Y^u_{ij}\bar{Q}_{Li}\epsilon\Phi^* U_{Rj} + \text{h.c.}, \tag{1.1}$$

where the Yukawa matrices, $Y^{u,d}$ are 3×3 complex matrices, Φ is the Higgs field, ϵ is the 2×2 antisymmetric tensor, and the labels i, j represent the generation indices. The left-handed quarks are represented by the doublet Q_L, and the right-handed quarks by the singlets U_R and D_R for the up and down types, respectively.

When the Higgs field acquires a vacuum expectation value (vev), the expectation value is no longer zero, $\langle H\rangle = (0, v/\sqrt{2})$ and the electroweak symmetry is spontaneously broken and mass terms are generated for the fermions.

The above lagrangian is written in the weak interaction basis. To obtain the physical masses of the particles it is necessary to perform a bi-unitary transformation on the Yukawa matrices to bring them to their diagonal form in the mass basis. Four unitary matrices are needed, $V^{u,d}_{L,R}$, and the diagonal mass matrix is given by

$$M^{u,d} = V^{u,d}_L\, Y^{u,d}\, V^{u,d\dagger}_R \left(\frac{v}{\sqrt{2}}\right). \tag{1.2}$$

In 1973 Kobayashi and Maskawa introduced a third generation of quarks to explain the observed CP violation [19]. This was an addition to the previous Cabbibo matrix that only incorporated the two generations of quarks known at the time. From the charged-current

weak interactions we can obtain what is called the CKM matrix given by

$$V_{\text{CKM}} \equiv V_L^u V_L^{d\dagger} = \begin{pmatrix} V_{ud} & V_{us} & V_{ub} \\ V_{cd} & V_{cs} & V_{cb} \\ V_{td} & V_{ts} & V_{tb} \end{pmatrix}. \tag{1.3}$$

The CKM matrix contains the parameter responsible for all CP-violating flavor-changing interactions, and the elements of the matrix are all fundamental parameters in the Standard Model and must be measured and inserted by hand.

It is easy to see the hierarchy present in the CKM matrix when written in what is called the Wolfenstein parametrization

$$\begin{pmatrix} 1-\frac{1}{2}\lambda^2 & \lambda & A\lambda^3(\rho - i\eta) \\ -\lambda & 1-\frac{1}{2}\lambda^2 & A\lambda^2 \\ A\lambda^3(1-\rho-i\eta) & -A\lambda^2 & 1 \end{pmatrix} + O(\lambda^4), \tag{1.4}$$

where $\lambda \approx 0.226$, $A = 0.814$, $\rho = 0.135$, $\eta = 0.349$ and CP-violation is encoded in the term $(\rho - i\eta)$.

As the CKM matrix describes the probability of transition from one quark type to another, with the probability proportional to $|V_{ij}|^2$, it is very clear that there is a strong hierarchy among the quark mixings, with no apparent explanation.

1.2.2 Baryon Asymmetry

As mentioned previously, the universe at present is made up of essentially only baryons and no antibaryons [15]. Why there is such a staggering asymmetry of baryons to antibaryons in

our universe is an outstanding problem in particle physics, and cannot be answered within the Standard Model, hinting at New Physics. Any process that produces a baryon asymmetry in the early universe is called baryogenesis.

The baryon asymmetry can be parametrized by η_B, which is the ratio of baryon to photon number densities. It is can be measured by studying Big Bang Nucleosynthesis and the Cosmic Microwave Background radiation, and is given by

$$\eta_b \equiv \frac{n_b}{n_\gamma} = 6.2 \times 10^{-10}. \tag{1.5}$$

In the early universe when temperatures were much higher (higher than a few hundred MeV) quarks and antiquarks were continually pair-created and annihilated in the quark-gluon plasma. This means that in the early universe, there existed approximately one unpaired quark per ten billion quark-antiquark pairs. At high temperatures the number of photons is about the same as the number of baryons, so the baryon asymmetry can be rewritten in terms of the number densities of quarks and antiquarks,

$$\frac{n_q - n_{\bar{q}}}{n_q + n_{\bar{q}}} \approx 10^{-10}, \tag{1.6}$$

where n_q and $n_{\bar{q}}$ is the number densities of quarks and antiquarks, respectively. This seemingly small asymmetry is responsible for our universe being composed of matter and not antimatter. This asymmetry was likely generated during the early universe at temperatures above 10^{10} GeV, in some sort of process where baryon number is not conserved. Then as the universe cooled, quarks and antiquarks annihilated, while the unpaired quarks remained, giving rise to the baryon asymmetry we see today.

It is reasonable to assume that when the universe began, there was no asymmetry between baryons and antibaryons, and that this asymmetry arose due to some process that did not

conserve baryon number. The problem of the baryon asymmetry is twofold: (1) understand where it came from; (2) understand its value. Since these two problems cannot be solved in the Standard Model, it is a very strong hint towards New Physics.

In 1967, Andrei Sakharov proposed a set of three necessary conditions that any baryon-generating process must satisfy simultaneously in order for it to produce baryons and antibaryons at different rates [20]. These are known as the Sakharov conditions. The conditions are:

- Violation of baryon number
- Violation of C and CP symmetries
- Departure from thermal equilibrium .

The justification for the first condition is relatively obvious, in that if the theory does not possess a mechanism for baryon number violation, it can produce no baryon asymmetry. The second condition is necessary because if charge conjugation symmetry is not violated, interactions which produce an excess of baryons over antibaryons will happen at the same rate as interactions which produce an excess of antibaryons over baryons, and again no asymmetry is left. CP-violation is similarly needed because otherwise left-handed baryons and right-handed antibaryons will be produced at the same rate as left-handed antibaryons and right-handed baryons. We can see this by studying the evolution of the density matrix,

$$\rho(t) = e^{-i\hat{H}(t-t_0)}\rho(t_0)e^{i\hat{H}(t-t_0)}, \tag{1.7}$$

where $\hat{H}$ is the Hamiltonian of the system, and t_0 is the initial time. If the system is C- and CP-invariant, the unitary operators U_C and U_{CP} corresponding to C- and CP-transformations, respectively, will commute with the Hamiltonian. In the case of CP-

invariance, for example, we have

$$U_{CP}\hat{H}U_{CP}^{-1} = \hat{H}, \tag{1.8}$$

which in terms of the density operator yields

$$U_{CP}\rho(t)U_{CP}^{-1} = \rho(t). \tag{1.9}$$

If the initial state is also CP-invariant, then the above is true at time t_0 as well. If we consider the fact that the baryon number operator, $\hat{B}$, is CP-odd, this means

$$U_{CP}\hat{B}U_{CP}^{-1} = -\hat{B} \tag{1.10}$$

which yields

$$\langle\hat{B}(t)\rangle = \mathrm{Tr}[\hat{B}\rho(t)] = 0, \tag{1.11}$$

which means the medium is baryon symmetric.

The departure from thermal equilibrium is necessary because if a system is in thermal equilibrium with respect to baryon number violating interactions, then the system has zero baryon chemical potential, which corresponds to zero baryon number density. Another way to think of this is that thermal equilibrium means that the conditions in the universe are time reversal symmetric (T). And since we are fairly confident CPT is a symmetry of nature, T and CPT together imply CP symmetry, which means that the number of baryons and antibaryons produced in the process would again be equal.

While the Standard Model does meet all three Sakharov conditions, the amount of baryon asymmetry is not enough to explain the observed asymmetry we see today. The main issue

is that the CP-violation induced by the CKM matrix is not nearly sufficient to generate the observed asymmetries. This is why BSM models must be considered.

In some baryogenesis mechanisms, the third criterion can be satisfied by the decay of heavy particles in an expanding universe. This is common in GUT baryogenesis models. In electroweak theory, this condition can be met if the electroweak phase transition is strongly first order, which proceeds via the nucleation of bubbles. Bubbles nucleate and expand out to eventually fill the entire universe, which causes the order parameter of the phase transition to change rapidly as the bubbles move outward, leading to a significant departure from thermal equilibrium.

The electroweak phase transition is not first order in the Standard Model, because the Higgs is much too heavy. It is instead a crossover which unfortunately does not satisfy Sakharov's third condition sufficiently. However, there are mechanisms that would allow the electroweak phase transition to be first order, the two we will be investigating presently are the addition of singlet scalar and large Yukawa couplings that vary during the phase transition.

1.3 Phase Transition Dynamics

Phase transitions occur when a symmetry of the ground state at zero temperature is not respected at higher temperatures. However, the symmetry can be restored at high temperatures [21]. As mentioned previously, at very high temperatures the electroweak symmetry, $SU(2)_L \times U(1)_Y$, was unbroken. As the temperature cooled, this symmetry was broken into $SU(2)_L \times U(1)_Y \to U(1)_{\text{em}}$. In the Standard Model, this phase transition proceeded via a crossover [22].

In order to study phase transitions, one must calculate what is called the effective potential, which is the free energy density of the system [23, 24]. In the case of the Higgs potential, at high temperatures after the Big Bang, the potential was symmetric, roughly resembling a parabola, with $\langle\phi\rangle = 0$. As the temperature cooled, a new minimum appeared, and the Higgs field eventually assumed this value at the new minimum where $\langle\phi\rangle \neq 0$. This can proceed via one of three ways, a first order phase transition, second order phase transition, or crossover.

A first order phase transition is associated with a discontinuity in the heat capacity and hence the order parameter at some temperature. A second order phase transition, on the other hand, has a continuous heat capacity (as a function of temperature), and hence no discontinuous jump in the value of the order parameter as the temperature changes.

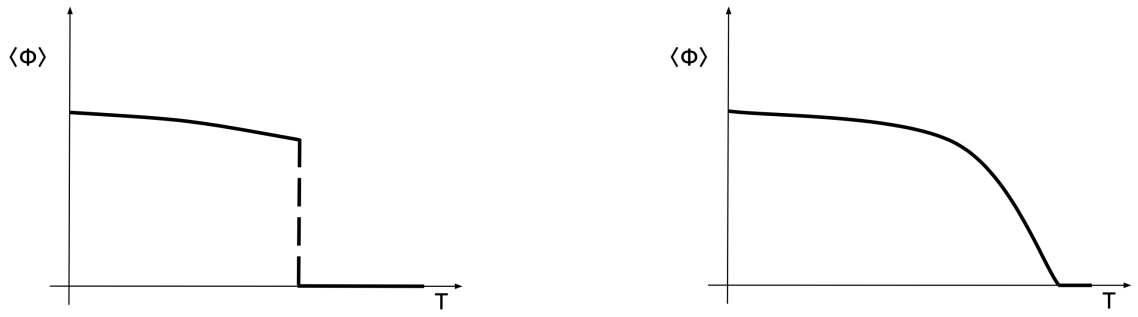

Figure 1.1: The heat capacity versus temperature for a first order (left) and second order (right) phase transition.

The distinction between first and second order transitions can be seen graphically below in Fig. 1.2. At high temperatures the potentials are symmetric, but as the temperature decreases, a new local minimum emerges at $\langle\phi\rangle \neq 0$. At a temperature called the critical temperature, T_c, the two local minima are equal, an the phase transition can proceed. Eventually the new minimum away from zero becomes the global minimum as the temperature

approaches zero. The potential associated with the first order phase transition generally develops a potential barrier separating the two local minima. The configuration must then tunnel from the $\langle\phi\rangle = 0$ false (metastable) minimum to the true global minimum via the nucleation of bubbles.

A first order phase transition proceeds via spontaneous nucleation of bubbles of new phase due to thermal fluctuations which allow tunneling to the energetically favorable global minimum. The bubbles percolate, expand, collide, and the system eventually returns to the homogeneous state of thermal equilibrium, but with $\langle\phi\rangle \neq 0$, and the released free energy is converted to heat.

A second order phase transition typically has no energy barrier between the two phases, and proceeds with the properties of the medium (in the case of the Higgs potential, $\langle\phi\rangle$) changing homogeneously from the symmetric phase to the broken phase. A second order phase transition produces no bubbles, since at every moment the system is in a state close to thermal equilibrium. A crossover is a bit more subtle, since in a crossover technically no phase transition occurs at all. The system slowly and smoothly shifts from one phase to the other, which happens over a region of phase space compared to at a specific point.

1.3.1 Electroweak Baryogenesis

Electroweak baryogenesis refers to any mechanism that produces an asymmetry between baryons and antibaryons during the electroweak phase transition in the early universe [1]. It has the added benefit of being both theoretically attractive and experimentally testable. Successful electroweak baryogenesis requires a strongly first order electroweak phase transition [25], which proceeds via nucleation of bubbles of broken phase into the unbroken

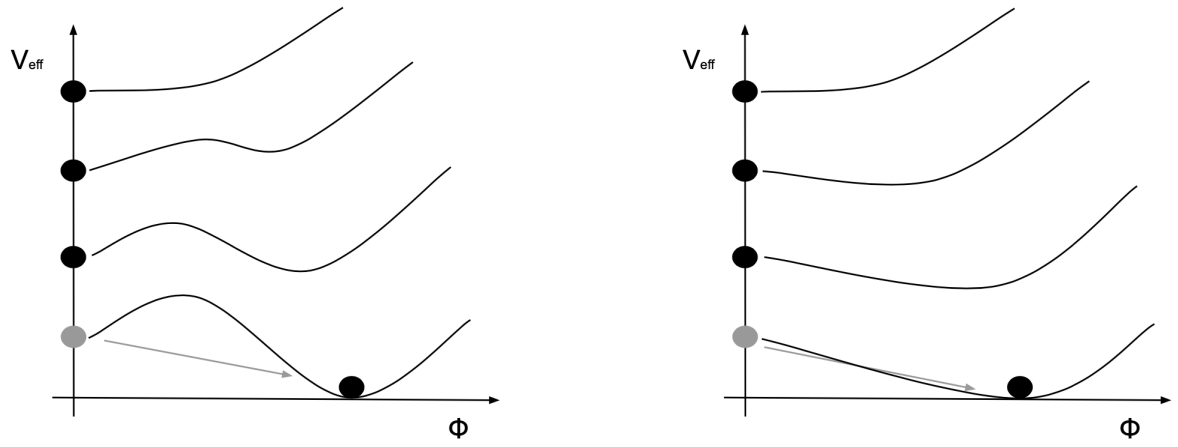

Figure 1.2: The effective potential (V_{eff}) at various temperatures for a first (left) and second (right) order phase transition.

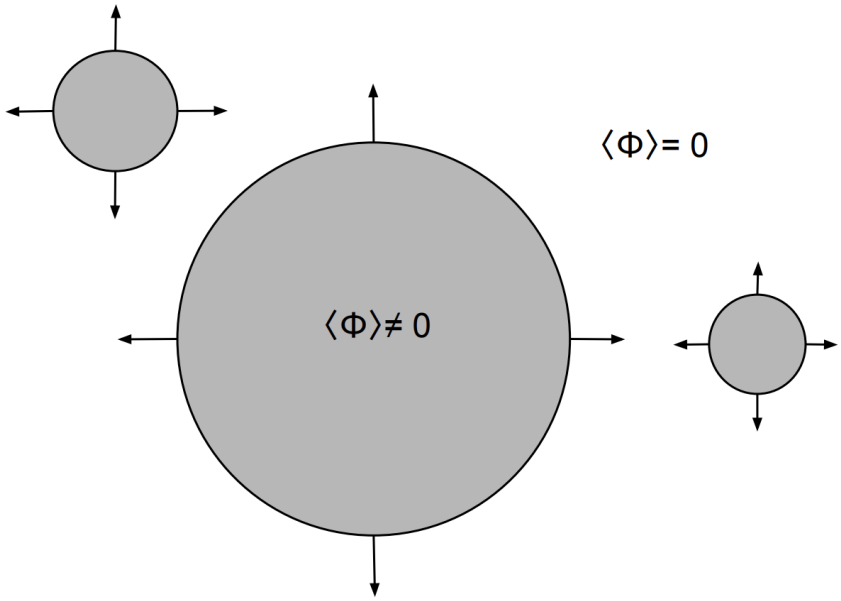

Figure 1.3: Bubbles of broken phase, where $\langle\phi\rangle \neq 0$, percolate and expand outward into the symmetric phase, eventually filling all of space.

phase until only broken phase remains. These bubbles are crucial for creating the desired baryon-antibaryon asymmetry in the universe and satisfying Sakharov's three conditions.

Besides adding new singlet scalars to the Standard Model, some other propositions to realize a first order electroweak phase transition include the 2-Higgs Doublet Model [26], and the

MSSM [27] (although which is now strongly disfavored).

One of the most powerful probes of beyond Standard Model CP-violation is the electric dipole moment of the electron [28]. Since the Standard Model prediction [29] for the electron EDM is impossibly small at current experiments, any detection at future experiments would be a smoking gun for new physics.

A first order electroweak phase transition can also produce a cosmological signal in the form of gravitational waves [30], which are created by the expansion and collisions of bubbles of broken phase during the phase transition. The signal is too low to be picked up by LIGO, but will likely be detectable by LISA in the future [31].

Chapter 2

The Effective Potential and Bubble Nucleation

2.1 The Effective Potential

Typically, calculations related to the electroweak phase transition are carried out using perturbation theory, however this method can be rife with uncertainties. A proper study of the phase transition must be done using Monte-Carlo methods, which are extremely computationally intensive. For many purposes, it suffices to use perturbation theory to gain an understanding of certain scenarios for electroweak baryogenesis.

The calculation of the effective potential is the main tool in studying phase transitions perturbatively. This method was developed [32, 33] using the path integral formalism. For a review, see [34]. The free energy density of a medium at temperature T and uniform Higgs field equal to $\langle\phi\rangle$ is called the effective potential. At zero temperature, the free energy reduces to the energy of the system (because quantum corrections are small) and the effective potential coincides with the scalar potential.

2.1.1 Calculation of the Effective Potential

The effective potential for a scalar field like the Higgs is given by the tree-level potential, plus one-loop zero temperature corrections, one-loop finite temperature corrections, and the daisy correction.

$$V_{\text{eff}}(\phi, T) = V_0(\phi) + V_1^{T=0}(\phi) + V_1^{T\neq 0}(\phi,\, T) + V_{\text{Daisy}}(\phi,\, T) \quad . \tag{2.1}$$

Both the zero temperature and finite temperature one-loop corrections receive contributions from all particles that couple to the Higgs, while the daisy correction receives contributions only from the bosons.

To compute the effective potential for the Standard Model of electroweak interactions, one starts with the tree level potential dependent on the Higgs field,

$$V_0(\phi) = -\frac{1}{2}\mu^2\phi^2 + \frac{\lambda}{4}\phi^4, \tag{2.2}$$

where there is a tree-level minimum at $v^2 = m^2/\lambda$. The electroweak symmetry is broken by the $SU(2)$ doublet

$$\Phi = \begin{pmatrix} \phi^+ \\ \phi^0 \end{pmatrix}, \tag{2.3}$$

which obtains a vev,

$$\langle\phi\rangle = \frac{1}{\sqrt{2}}\begin{pmatrix} 0 \\ v \end{pmatrix}. \tag{2.4}$$

The Higgs mass is then given by

$$m_h^2(\phi) = 3\lambda\phi^2 - \mu^2, \tag{2.5}$$

so that at the vev the Higgs mass is $m_h^2(v) = 2\lambda v^2 = 2\mu^2$. The weak gauge boson masses are given by

$$m_W^2(\phi) = \frac{g_2^2}{4}\phi^2, \tag{2.6}$$

$$m_Z^2(\phi) = \frac{g_2^2 + g_Y^2}{4}\phi^2. \tag{2.7}$$

where g_2 and g_Y are the weak and hypercharge coupling constants.

The fermion masses are also dependent on the value of the Higgs field, and are given by

$$m_f^2(\phi) = \frac{y_f^2}{2}\phi^2, \tag{2.8}$$

where y_f is the Yukawa coupling for each fermion. However, only the top quark will contribute significantly to the one-loop effective potential due to its large Yukawa coupling, as other fermions have negligible couplings and hence their contributions are also negligible.

The one-loop correction to the scalar potential at zero temperature is obtained by summing over all one particle irreducible (1PI) diagrams with one loop and zero external momenta, as displayed in Fig. 2.1

The details of the calculation are given in appendix B.2, and can be generalized to any number of complex scalar fields. After renormalizing using the $\overline{\text{MS}}$ scheme, the one-loop

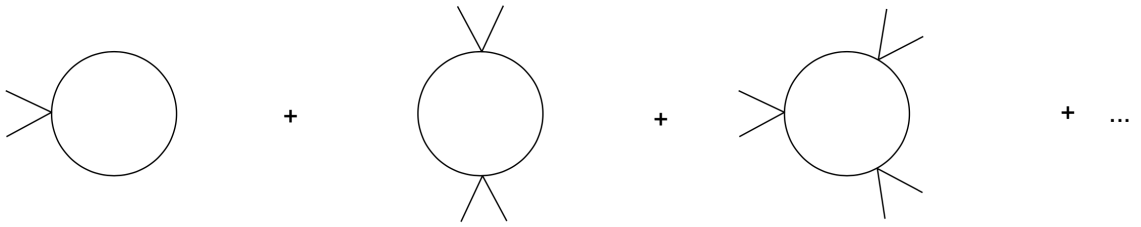

Figure 2.1: 1PI diagrams contributing to the one-loop effective potential.

zero temperature contribution is given by

$$V_1^{T=0}(\phi) = \sum_i \frac{n_i(-1)^{F_i}}{64\pi^2}\left[m_i^4(\phi)\left(\log\left[\frac{m_i^2(\phi)}{m_i^2(v)}\right] - \frac{3}{2}\right) + 2m_i^2(\phi)m_i^2(v)\right] , \tag{2.9}$$

where the sum is over all particles that couple to the Higgs. F is 0 or 1 for bosons and fermions, respectively, and n_i is the particle's multiplicity (1 for each boson, 4 for colorless Dirac fermions, and 12 if the fermion also carries color). This expression already includes all counter-terms necessary to maintain the tree-level values of the mass and coupling constant.

To calculate the finite temperature contributions, the same procedure is carried out as for the zero temperature correction, but instead using the finite temperature Feynman rules when summing over all 1PI diagrams. This yields

$$V_1^{T\neq 0}(\phi, T) = \sum_i \frac{n_i(-1)^{F_i}T^4}{2\pi^2} J_{\mathrm{B/F}}\left(\frac{m(\phi)^2}{T^2}\right) , \tag{2.10}$$

where $J_{B/F}$ is the thermal bosonic or fermionic function given by

$$J_{B/F} = \int_0^\infty dx\, x^2 \log\left[1 - (-1)^F e^{-\sqrt{x^2 + m^2/T^2}}\right] . \tag{2.11}$$

This integral has convenient high temperature approximations for $m^2/T^2 \ll 1$, allowing us

to rewrite the thermal bosonic and fermionic function as

$$J_{\rm B}\left(\frac{m^2}{T^2}\right) = -\frac{\pi^4}{45} + \frac{\pi^2}{12}\frac{m^2}{T^2} - \frac{\pi}{6}\left(\frac{m^2}{T^2}\right)^{3/2} - \frac{1}{32}\frac{m^4}{T^4}\log\left(\frac{m^2}{a_b T^2}\right) \ , \tag{2.12}$$

$$J_{\rm F}\left(\frac{m^2}{T^2}\right) = \frac{7\pi^4}{360} - \frac{\pi^2}{24}\frac{m^2}{T^2} - \frac{1}{32}\frac{m^4}{T^4}\log\left(\frac{m^2}{a_f T^2}\right) \ , \tag{2.13}$$

where $\ln a_b = 5.4076$ and $\ln a_f = 2.6351$, and the mass dependence on ϕ is understood.

2.1.2 The Daisy Correction

The existence of symmetry restoration implies a failure of perturbation theory at high temperatures [35]. Since the tree-level potential, which is not temperature dependent, has broken symmetry, temperature-dependent radiative corrections should not be able to restore the symmetry. The one-loop approximation is valid at temperatures below the critical temperature; however, near the critical temperature this approximation breaks down.

Quadratically divergent loops that add a factor of $\lambda T^2/m^2$ to the two-point functions can be safely ignored at low temperatures where $\lambda T^2/m^2 \ll 1$. At and above the critical temperature, these divergent diagrams (called daisy, or sometimes ring diagrams) cannot be safely ignored and must be accounted for by resumming over an infinite number of diagrams at every order. This is equivalent to replacing the particle mass by an effective mass, $m^2 \to m^2 + \Pi(T)$, where $\Pi(T)$ is the thermal mass of the particle. Physically, this means as the particle propagates in the medium, it can interact with the background distribution of particles, thereby increasing the effective mass of the particle.

Again considering a self-interacting real scalar field, a loop amplitude with divergence D will be of the form $T^D f(m/T)$, and absent any infrared divergences as m/T approaches zero the loop will go like T^D. For example, the diagram in Fig. **??**, which contributes to the self energy, has divergence $D = 2$ and thus scales like λT^2.

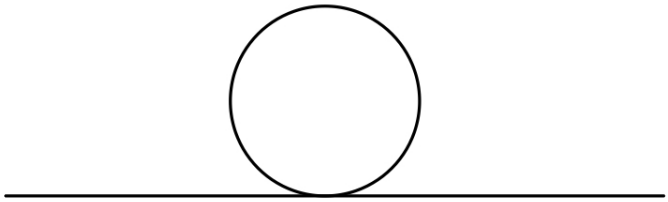

Figure 2.2: One-loop contribution to the self energy of a scalar field, scales like λT^2.

If the divergence is less than or equal to zero, infrared divergences appear in the bosonic propagators when summing over the Matsubara zero modes (see Appendix C for details). In these cases there is only one factor of T, so every logarithmically divergent loop contributes a factor of T. For example, the diagram in Fig. 2.3 has two logarithmically divergent loops and thus contributes a factor of $\lambda^2 T^2$. These graphs, as we will see, are suppressed by a factor of λ compared to the daisy diagrams, and can be ignored.

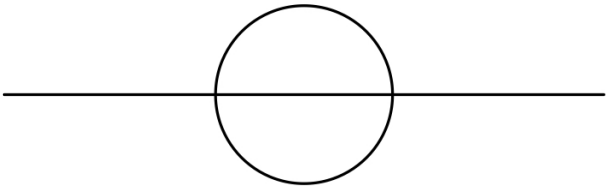

Figure 2.3: Two-loop contribution to the self-energy for the scalar theory. This diagram is suppressed by a factor of λ compared to the one-loop diagram.

We can now see that the diagrams with the largest contributions will be the diagrams with the largest number of quadratically divergent loops. If we take the diagram in Fig. **??**, and add n loops on top of it, we will have an additional contribution of $(\lambda T^2)^n$.

If we rescale the contributions according the mass scale of the theory, M, each additional

quadratically divergent loop adds a factor of $\lambda T^2/M^2$. In order for the one-loop approximation to be valid we need to have this factor much less than one. However, at the critical temperature we know this is not true, so we can see now that the one-loop approximation is not valid at high temperatures near the critical temperature. We can no longer safely ignore these quadratically divergent diagrams. The solution is to re-sum all powers of $\lambda T^2/M^2$ into a thermal mass term, and replace the mass by an effective mass.

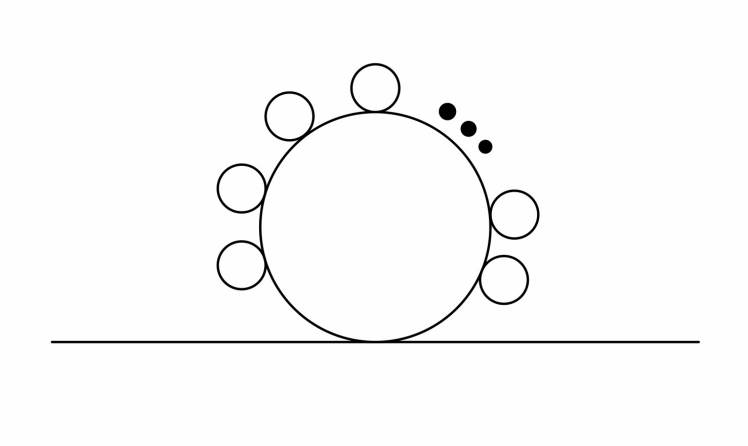

Figure 2.4: Daisy contribution to the self energy which cannot be ignored at high temperatures.

After resumming over the Matsubara zero modes that produce the infrared divergence, we obtain

$$V_{\text{Daisy}}(\phi, T) = \sum_i \frac{n_i T}{12\pi} \left(m_i^3(\phi) - \left[m_i^2(\phi) + \Pi_i(T) \right]^{3/2} \right), \tag{2.14}$$

for the daisy contribution.

In the case of the Higgs, the thermal mass is given by [36]

$$\Pi_\phi(T) = \left(\frac{3}{16} g_2^2 + \frac{1}{16} g_y^2 + \frac{\lambda}{2} + \frac{y_t^2}{4} \right) T^2 , \tag{2.15}$$

where y_t is the top quark Yukawa coupling. Only the top quark contribution to the Higgs is included here since it is much larger than all the others. We will see in later sections that when the other Yukawa couplings are large, their contribution to the Higgs thermal mass must be included.

The daisy correction is especially important when studying first order phase transitions because it affects the cubic term in the effective potential, which is the term responsible for the potential barrier. For example, if the thermal mass is large relative to the mass squared, the potential ceases to behave as a cubic term in ϕ and the phase transition is no longer necessarily first order.

2.2 A Simple Phase Transition

Now that we have completed our calculation of the effective potential, it is helpful to illustrate with a simple example the difference between first and second order phase transitions. One can write the effective potential in a simplified approximate form using the high temperature expansions of the thermal bosonic and fermionic functions. This gives

$$V_{eff}(\phi, T) \approx D(T^2 - T_0^2)\phi^2 - ET\phi^3 + \frac{\bar{\lambda}}{4}\phi^4, \tag{2.16}$$

where D and $\bar{\lambda}$ are slowly varying functions of temperature, and can be assumed to be constant. At zero temperature, the point at $\phi = 0$ is unstable, and the minimum at $\phi(0) = \pm\sqrt{\frac{2D}{\lambda}}T_0$ is the global minimum and hence a stable minimum. If the coefficient E is zero, corresponding to the cubic term in ϕ, the phase transition is second order at a temperature of T_0. This is because without the cubic term, there is no potential barrier between the symmetric and broken phase. The Higgs expectation value for temperatures below the

critical temperature is then given by

$$\langle\phi\rangle = T_0\sqrt{\frac{2D}{\bar{\lambda}}\left(1-\frac{T^2}{T_0^2}\right)}. \tag{2.17}$$

If the coefficient E is nonzero, this cubic term in ϕ can yield a first-order phase transition by creating a potential barrier between the symmetric and broken phases. As the temperature cools from very high temperatures where the potential is in the symmetric phase, a second local minimum begins to develop at $\phi \neq 0$, at a temperature T_1 of

$$T_1 = T_0\sqrt{\frac{8\bar{\lambda}D}{8\bar{\lambda}DT_0^2 - 9E^2}}. \tag{2.18}$$

The temperature at which the new local minimum decreases to the same value as the minimum at the origin is the critical temperature, T_c, and the phase transition can now occur. This minimum continues to descend, and at zero temperature it is the true global minimum. This new minimum is at ϕ_c and given by

$$\frac{\phi_c}{T_c} = \frac{2E}{\bar{\lambda}}. \tag{2.19}$$

where the phase transition can begin at T_c via tunneling through the barrier between the symmetric and broken phases. If the barrier is very high, the tunneling probability is very small and tunneling may start at a lower temperature. In some cases, as we will see, this stops tunneling from occurring at all, and there is no phase transition.

2.3 Bubble Nucleation

First-order cosmological phase transitions proceed via the nucleation of bubbles of true vacuum out of metastable false vacuum states. Inside the bubble, the free energy density is lower than the free energy density outside the bubble; if a bubble is too small, the surface tension is too great and the bubble collapses; if the bubble is sufficiently large it will expand and convert the medium to the new phase. If the internal pressure of the bubble is sufficient to counterbalance the surface tension, the bubble will expand. The minimum bubble size that can begin to expand is called the critical bubble, and it is these bubbles that will drive the phase transition.

The formalism of bubble nucleation in cosmological phase transitions was developed in [37] (for further information on tunneling, see [38]). The tunneling rate, or bubble nucleation rate, is determined by the euclidean action. Start first with a lagrangian

$$\mathcal{L} = \frac{1}{2}\left(\partial_\mu\phi\partial^\mu\phi - V(\phi)\right), \tag{2.20}$$

where the euclidean action is given by

$$S_E = \int \left(\frac{1}{2}\left(\partial_\mu\phi\right)^2 + V(\phi)\right) d^dx. \tag{2.21}$$

The dimension d is 4 for zero temperature and 3 for finite temperature tunneling. Bubbles will nucleate when the probability per unit time per unit volume that the false vacuum will decay is order one. The bubble nucleation rate per unit volume is given by

$$\frac{\Gamma}{V} \sim A(T)e^{-S_E}, \tag{2.22}$$

at zero temperature, where $A(T)$ is a slowly varying, and is typically quite difficult to solve and must be done numerically. At finite temperatures the nucleation rate per unit volume

is given by

$$\frac{\Gamma}{V} = Ae^{-S_E/T}. \tag{2.23}$$

At high temperatures, the action's $O(4)$ symmetry becomes an $O(3)$ symmetry, and the euclidean action simplifies to

$$S_3 = 4\pi \int_0^\infty d\rho\rho^2 \left[\frac{1}{2}\left(\frac{d\phi}{d\rho}\right)^2 + V(\phi(\rho), T)\right], \tag{2.24}$$

where ρ is the usual spherical coordinate.

The corresponding equations of motion for the critical bubble are

$$\frac{d^2\phi}{d\rho^2} + \frac{2}{\rho}\frac{d\phi}{d\rho} = V'(\phi, T). \tag{2.25}$$

This is identical to a classical particle moving in an inverted potential, $-V(\phi)$. The solution to the critical bubble profile can then be solved by the "overshoot-undershoot" method described in [39].

For the overshoot-undershoot method, we take a particle rolling on the inverted potential, and find an initial placement near the true vacuum, ϕ_T, (global maximum in the inverted case) such that when the particle rolls down the potential it stops at the point corresponding to the false vacuum, ϕ_F. One then varies the initial placement of the particle; if it "overshoots," or rolls past the false vacuum, the initial placement must be placed a bit further from the true vacuum. If instead the particle does not reach the false vacuum as it rolls down the potential, it "undershoots," the next iteration must place the initial condition closer to the true vacuum. The corresponding configuration is usually called the bounce solution.

Once we establish the critical radius of a bubble large enough to grow after formation, the

subsequent progress of the phase transition depends on the ratio of the rate of production of bubble to the expansion rate of the universe. At the electroweak scale this corresponds to a bubble nucleation rate of order unity when

$$\frac{S_E}{T} \approx 140. \tag{2.26}$$

(There is some discrepancy in this result, with some sources citing as low as ~ 100 [40]. We will be using 140 in this analysis.)

2.3.1 Generation of Baryon Asymmetry

The vacuum structure of non-abelian gauge theories has non-trivial vacuum gauge configurations which, in the case of the electroweak theory leads to the anomalous non-conservation of baryon number. Transitions between different vacua are accompanied by a change in the baryon number, albeit these are highly suppressed at zero temperature. However, at finite temperature these transitions can be possible via thermal effects.

Thermal fluctuations in the $SU(2)$ gauge field and symmetry breaking Higgs field can cause transitions between degenerate minima with different baryon numbers separated by a potential barrier. The transitions may actually proceed over the potential barrier between different vacua, and the maximum free energy for the transition corresponds to a static, unstable field configuration at the top of the barrier called a sphaleron [41].

The sphaleron solution is a saddle point in the field configuration space, representing the lowest barrier between two neighboring vacuums, and hence classically unstable.

In [42] it was argued that the barrier separating vacua may be surmounted at temperatures

around 100 Gev, so this is relevant for electroweak physics.

Sphalerons can "washout" any baryon asymmetry created during a phase transition if the phase transition is not strongly first order. Taking into account the baryon violation rate and the probability of fluctuations over the barrier, in order for a phase transition to be viable [43, 44] in electroweak baryogenesis it must satisfy

$$\frac{\phi_c}{T_c} \gtrsim 1.0, \tag{2.27}$$

where T_c is the critical temperature and ϕ_c is the expectation value of the Higgs field at that temperature.

As mentioned previously, in order for any model to generate baryon asymmetry, it must satisfy the three Sakharov conditions simultaneously. In our case, electroweak baryogenesis satisfies the out of equilibrium criteria with a first order phase transition. However, the CP-violation in the Standard Model CKM matrix is not sufficient to produce the baryon asymmetry we observe today, so some other mechanism must be present to provide sufficient CP-violation.

The first order phase transition can satisfy both the second and third of Sakharov's conditions. During the phase transition the value of the Higgs field is changing, and is when the departure from thermal equilibrium takes place and when C- and CP-violation takes place. The creation of baryons during electroweak baryogenesis takes place near of bubble walls, as explained in [2].

Particles in the cosmic plasma scatter off the bubble walls which can generate violations of C- and CP-symmetry in front of the bubble wall. CP-violation comes into play when chiral fermions scatter off the Higgs at the bubble wall. This is a kinetic effect as particles inside the bubble are massive, while particles outside the bubble are massless. A chiral asymmetry

is created in front of the bubble wall that is converted by sphalerons into a baryon number. These asymmetries then bias electroweak sphaleron transitions to produce more baryons than antibaryons as the bubble wall expands. As the bubbles expand, some of the baryon excess created outside the bubble is swept up by the expanding bubble into the broken phase.

Chapter 3

Electroweak Phase Transition with Varying Yukawa Couplings

A scenario was proposed in [9] that a first order electroweak phase transition can be obtained if the Yukawa coupling constants varied as the universe evolved. Order one Yukawa couplings were assumed before the phase transition, which then decrease to assume their present values during the phase transition. This proposal utilized the Froggatt-Nielsen mechanism to implement the variation in the Yukawa couplings, and has the benefit of addressing both the flavor problem and the matter-antimatter asymmetry. The Froggatt-Nielsen mechanism was originally proposed as a solution to the flavor problem, however; this mechanism could affect the dynamics and cosmology of the early universe which has not been studied in much depth.

3.1 The Froggatt-Nielsen Mechanism

The Froggatt-Nielsen Mechanism [45] assumes a new $U(1)_{FN}$ flavor symmetry under which the fermions are charged. This symmetry is broken by a new scalar field called the "flavon," which acquires a vev to break the $U(1)$ flavor symmetry, and is typically a Standard Model singlet. If the left- and right-handed fields have different charges under $U(1)_{FN}$, the effective Yukawa couplings of the fermions are generated by higher dimensional operators when the flavon field obtains a vev. The effective Yukawas couplings are dependent on the flavon vev and are of the form $(Y\langle S\rangle/M)^n$, where the scale of new physics is $\Lambda = M/Y$ and $\langle S\rangle$ is the vev of the flavon, and M is the mass scale.

The hierarchy observed in the Standard Model Yukawa couplings is then derived from differing powers of $\langle S\rangle/\Lambda$. The lagrangian of this theory with a single additional flavon is given by

$$\mathcal{L} = \tilde{y_{ij}} \left(\frac{S}{\Lambda}\right)^{\tilde{n}_{ij}} \bar{Q}_i \tilde{\Phi} U_j + y_{ij} \left(\frac{S}{\Lambda}\right)^{n_{ij}} \bar{Q}_i \Phi D_j, \tag{3.1}$$

where Q_i is the Standard Model quark doublet, U_i and D_i are the right handed up and down type quarks, respectively, and the subscript i denotes the generation. The Higgs boson is denoted by Φ ($\tilde{\Phi} = i\sigma_2\Phi^*$), and y_{ij} are order one dimensionless couplings. The values of n_{ij} and $\tilde{n}_{ij}$ are chosen such that the terms are singlets under the new $U(1)$ flavor symmetry.

Once the symmetry breaks and the flavon obtains a vev, the lagrangian looks like

$$\mathcal{L} = \tilde{y_{ij}} \left(\frac{v_s}{\sqrt{2}\Lambda}\right)^{\tilde{n}_{ij}} \bar{Q}_i \tilde{\Phi} U_j + y_{ij} \left(\frac{v_s}{\sqrt{2}\Lambda}\right)^{n_{ij}} \bar{Q}_i \Phi D_j, \tag{3.2}$$

where $y_{ij}\left(\frac{v_s}{\sqrt{2}\Lambda}\right)$ now plays the roll of the Yukawa coupling in the mass basis. We can see

that in the mass basis the effective Yukawa couplings now have a clear hierarchy, and let

$$\epsilon \equiv \frac{v_s}{\sqrt{2}\Lambda}. \tag{3.3}$$

Now we can see that the effective Yukawa couplings are determined solely by powers of $(\epsilon_f)^{n_f}$, where n_f is appropriately chosen to give the particle's observed Yukawa coupling.

For example, making a typical assignment of Froggatt-Nielsen charges to the quarks

$$\begin{array}{lll} \bar{Q}_3 : 0 & \bar{Q}_2 : +2 & \bar{Q}_1 : +3 \\ U_3 : 0 & U_2 : +1 & U_1 : +4, \\ D_3 : +2 & D_2 : +2 & D_1 : +3 \end{array} \tag{3.4}$$

for the effective Yukawa couplings in terms of powers of ϵ this yields

$$\begin{array}{lll} y_t \sim 1 & y_c \sim \epsilon^3 & y_u \sim \epsilon^7 \\ y_b \sim \epsilon^2 & y_s \sim \epsilon^4 & y_d \sim \epsilon^6. \end{array} \tag{3.5}$$

One can also rewrite the entries of the CKM matrix in terms of powers of ϵ. This mechanism allows the mass and mixing hierarchies to be explained as powers of the expansion parameter, rather than assigning seemingly arbitrary Yukawa couplings for each fermion. This also means that the mechanism does not depend on the scale of the new physics, only on the ratio $\frac{\langle S \rangle}{\Lambda}$.

3.2 Varying Yukawa Couplings

It was proposed in [9], that a first order electroweak phase transition can be achieved by varying the Yukawa couplings throughout the phase transition. An analysis of the effective potential and phase transition with varying Yukawa couplings was carried out, where the Yukawa couplings are taken to be order one before the electroweak phase transition, then assume their observed Standard Model values after the phase transition.

A simple ansatz was used to account for this variation in the Yukawa couplings,

$$y(\phi) = \begin{cases} y_1 \left(1 - \frac{\phi}{v}\right)^n + y_0 & 0 \leq \phi \leq v \\ y_0 & v \leq \phi \ , \end{cases} \tag{3.6}$$

where ϕ is the value of the Higgs field, y_1 is a constant of order one, and n simply controls how quickly the Yukawa couplings change throughout the phase transition. The constant y_0 corresponds to the present value of the Yukawa for a given fermion. For a simple toy-model analysis, a value of $y_0 = 0.02$ for all quarks was assumed.

In this case, the mass of the fermions would also depend on the Higgs vev through $y(\phi)$, and can take the form

$$m_f(\phi) = \frac{y(\phi)\phi}{\sqrt{2}}. \tag{3.7}$$

which would mean the masses of the fermions could vary significantly during the phase transition. If additional scalars are added, then the mass of the fermions can also be dependent on powers of the vev of those scalars, to be seen in later sections.

This addition of varying the Yukawa couplings greatly changes the dynamics of the phase

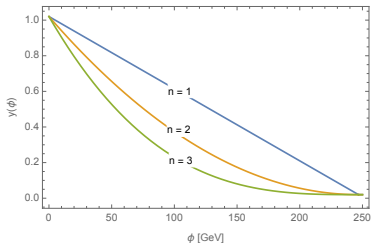

(a) Varying Yukawa couplings given various values of n.

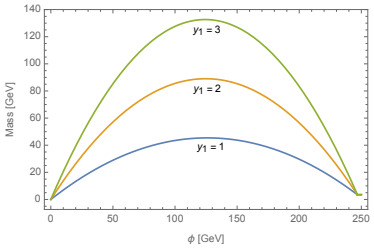

(b) Fermion mass with varying y_1, and $n = 1$ held constant.

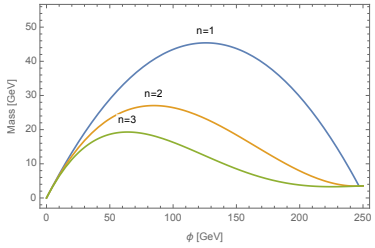

(c) Fermion mass with $y_1 = 1$ held constant, varying n.

Figure 3.1: Yukawa couplings and fermion masses with varying values of y_1 and n.

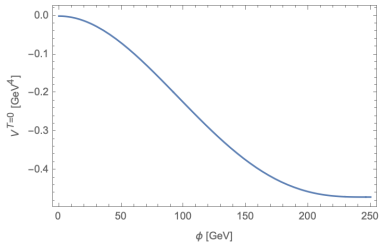

(a) Standard Model contribution, i.e. constant Yukawa couplings.

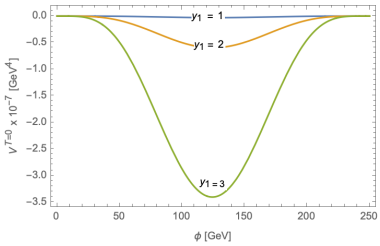

(b) Contribution with varying y_1, $n = 1$ held constant.

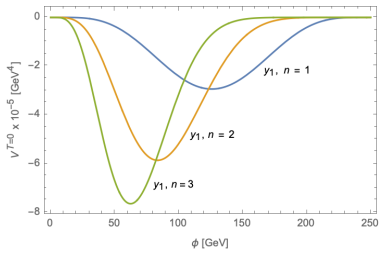

(c) Contribution with varying y_1 and varying n.

Figure 3.2: Zero temperature one-loop fermion contribution to the effective potential with varying y_1 and n.

transition, particularly the finite temperature contributions of the fermions.

Below are the contributions for a fermion with varying n and $y1$ versus constant Yukawa couplings. As can be seen, the contributions change significantly.

The finite temperature contributions are naturally also impacted. This contribution is the most important now for generating a first order phase transition because the variation in the Yukawas creates the crucial cubic term in the potential.

If one studies the high temperature approximation of the thermal fermionic function,

$$J_f\left(\frac{m^2(\phi)}{T^2}\right) \approx \frac{7\pi^2}{360} - \frac{\pi^2}{24}\frac{m_f^2(\phi)}{T^2} - \frac{1}{32}\frac{m_f^4(\phi)}{T^4}\text{Log}\left[\frac{m_f^2(\phi)}{13.9T^2}\right], \tag{3.8}$$

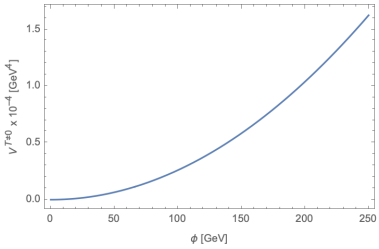

(a) Standard Model finite temperature fermion contribution.

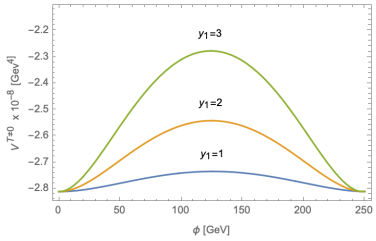

(b) Contribution with varying y_1, n held constant at $n = 1$.

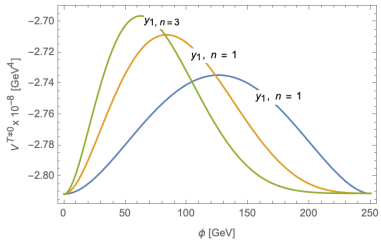

(c) Contribution with varying y_1 and n.

Figure 3.3: Finite temperature one-loop fermion contribution to the effective potential, with varying y_1 and n.

we see that it can give rise to a cubic term. Since the mass is now dependent on the Yukawa couplings which are varying, this means the second term in the thermal fermionic function has a dependence on ϕ^3

$$m^2(\phi) = \frac{y^2(\phi)\phi^2}{2} \propto \left(1 - \frac{2\phi}{v} + \frac{\phi^2}{v^2}\right)\phi^2\,, \tag{3.9}$$

and so we have the necessary ϕ^3 term for a first order phase transition where there previously was none.

The Higgs thermal mass and hence the daisy contribution from the Higgs is also affected. The thermal mass now is a funciton of ϕ, whereas previously it was a constant value. The Higgs thermal mass in the Standard Model, including only the top quark contribution due to its large coupling is given by

$$\Pi_\phi(\phi, T) = \left(\frac{3}{16}g_2^2 + \frac{1}{16}g_y^2 + \frac{\lambda}{2} + \frac{y_t}{4}\right)T^2\,, \tag{3.10}$$

whereas with varying Yukawa couplings all of the fermions which couple to the Higgs must be included (since they now have large couplings before the phase transition) and is given

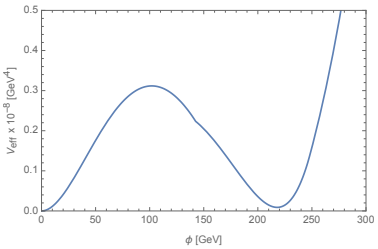

(a) Effective potential with $y_1 = 1$.

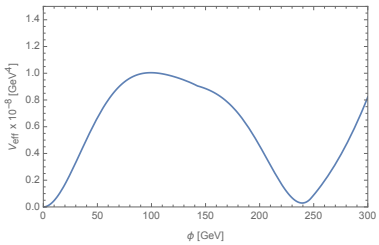

(b) Effective potential with $y_2 = 2$.

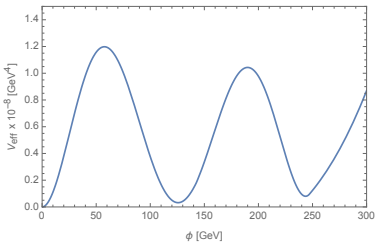

(c) Effective potential with $y_1 = 3$.

Figure 3.4: The effective potential at the critical temperature with varying Yukawa couplings, n held constant at $n = 1$.

by

$$\Pi_\phi(\phi, T) = \left(\frac{3}{16} g_2^2 + \frac{1}{16} g_y^2 + \frac{\lambda}{2} + \frac{y_t}{4} + \frac{n_i y_i(\phi)}{4} \right) T^2 \tag{3.11}$$

where n_i is the degrees of freedom for the remaining fermions and y_i are their Yukawa couplings.

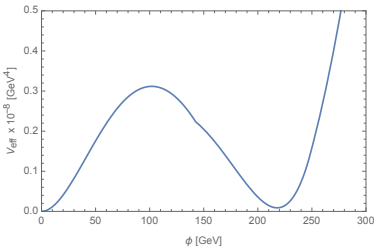

(a) Effective potential with $n = 1$.

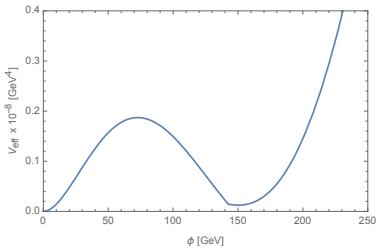

(b) Effective potential with $n = 2$.

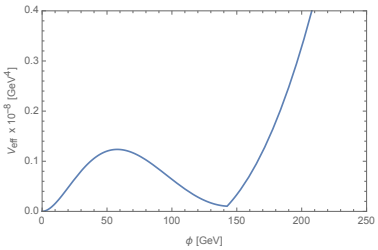

(c) Effective potential with $n = 3$.

Figure 3.5: Effective potential at the critical temperature with varying Yukawa couplings, physical masses, and $y_1 = 1$ for all and varying values of n.

The overall effect of allowing the Yukawa couplings to vary during the phase transitions is twofold: the first is the most significant, changing the phase transition from second to first order, and the other is decreasing the critical temperature. As mentioned previously, a first order phase transition suitable for electroweak baryogenesis must satisfy $\phi_c/T_c \gtrsim 1.1$, which the case of varying Yukawa couplings with $y_1 = 2.0$ and $y_0 = 0.02$ satisfies. The switch from

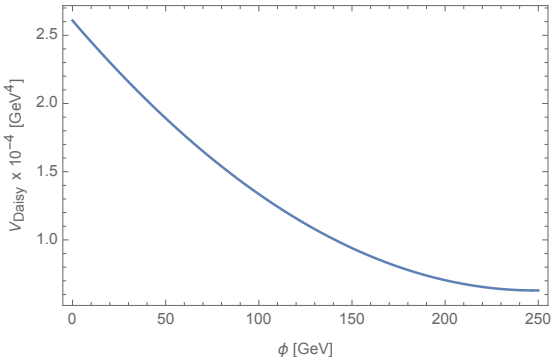

(a) Higgs thermal mass with varying Yukawa couplings.

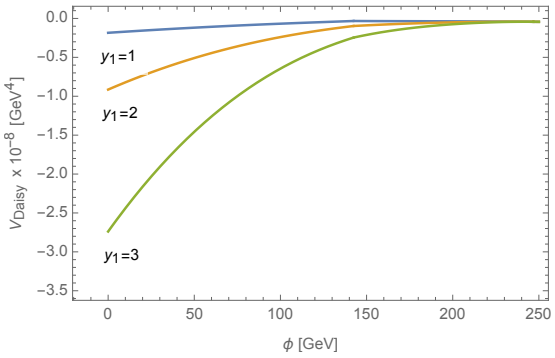

(b) Daisy contribution with varying values of y_1 and $n = 1$.

Figure 3.6: Higgs thermal mass and daisy contribution in the case of varying Yukawas.

second to first order is clearly the most important to early universe cosmology, as a first order phase transition is necessary for electroweak baryogenesis.

Overall, if the Yukawa couplings vary during the electroweak phase transition, the phase transition undergoes two main changes. First, the finite temperature one-loop contributions from the fermions creates a cubic term in ϕ and thus a potential barrier between the symmetric and broken phases where previously there was none. This can result in a first-order phase transition. Second, large Yukawa couplings at $\phi \sim v$ increase the Higgs thermal mass, which lowers the potential close to $\phi = 0$ through the Daisy correction. The net result of these effects is to create a first-order phase transition in what was previously a crossover.

3.3 Stability of a Theory with Varying Yukawas

In the Standard Model, the Higgs quartic coupling becomes negative around 10^{10} GeV, rendering the Higgs potential unstable. Increasing the number of Yukawa couplings that are of order one drastically lowers the scale at which the quartic coupling becomes negative [46].

This can be seen analytically from the 1-loop β function (equation A.3 in appendix A). If we assume only one large quark Yukawa coupling and no CKM mixing, then the leading order terms can be approximated as

$$\beta_\lambda^{(1)} \approx 24\lambda^2 + 12\lambda y^2 - 6y^4 \ . \tag{3.12}$$

If additional quark Yukawa couplings of order one are added, the β function becomes

$$\beta_\lambda^{(1)} \approx 24\lambda^2 + 12\lambda n y^2 - 6n y^4 \ , \tag{3.13}$$

where n is the number of order one Yukawa couplings. The addition of these large Yukawa couplings will make the negative term dominant, driving the Higgs quartic coupling negative at a lower scale. Here, the effects of the large Yukawa couplings on the evolution of $\beta_\lambda^{(1)}$ is independent of the specific variation used in the Yukawa couplings, and can include a broad range of models where the additional scalar fields are heavy. In the case of additional light scalars, the beta functions will need to be calculated (dependent on the model) to incorporate those effects.

To evaluate the full renormalization group equations (RGEs) with large Yukawa couplings, and their effect on the running of the Higgs quartic coupling, the Mathematica package SARAH [47] was used. In Figure 3.7, the number of Yukawa couplings equal to 1.0 were successively increased at the electroweak scale. The top quark Yukawa coupling and all other parameters were kept at their Standard Model values. It is clear that this drastically lowers the scale at which the Higgs quartic coupling becomes negative, pushing it very close to the electroweak scale.

In the next case considered, the order one Yukawa couplings are imposed at 1 TeV. Figure 3.8 has Yukawa couplings equal to 1.0 and 2.0. As shown in the figures, setting the Yukawa

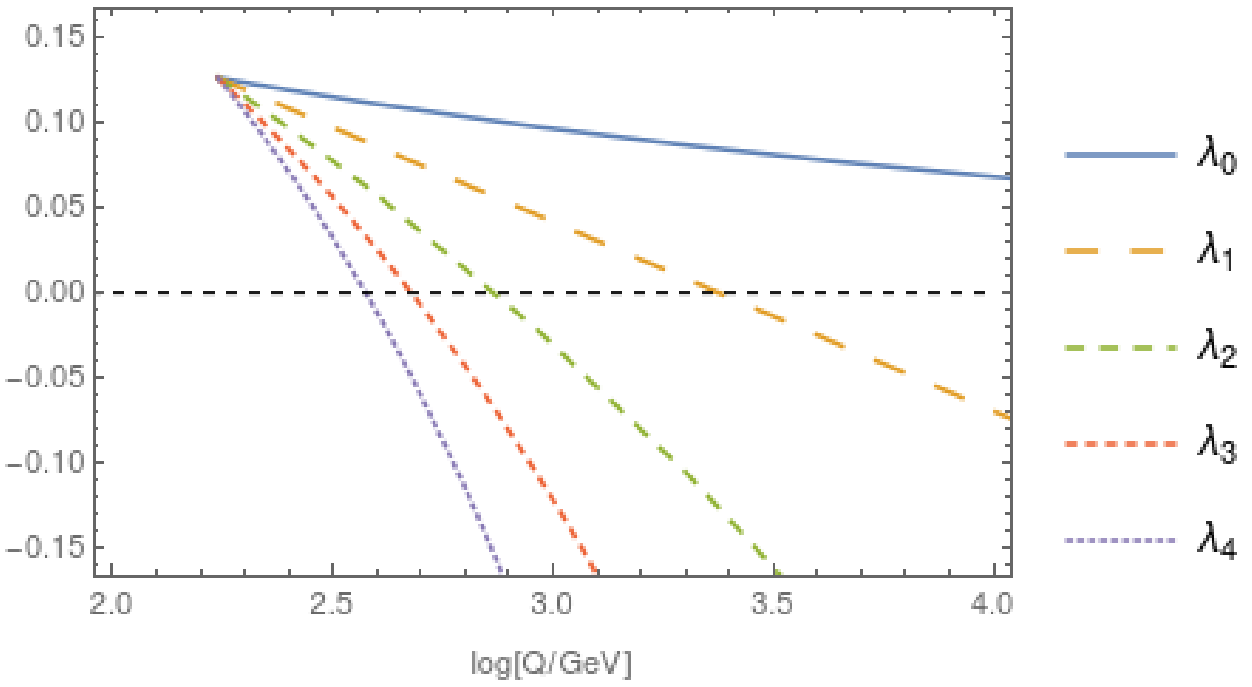

Figure 3.7: RGE running of the Higgs quartic coupling with additional Yukawa couplings equal to 1.0, and Standard Model boundary conditions imposed at the electroweak scale. The number of additional Yukawa couplings is given by n, with $n = 0$ corresponding to the case of the Standard Model.

couplings to be order one or greater increases the Higgs quartic coupling at the electroweak scale. This in turn has the effect of lowering the Higgs mass, as seen in the following section.

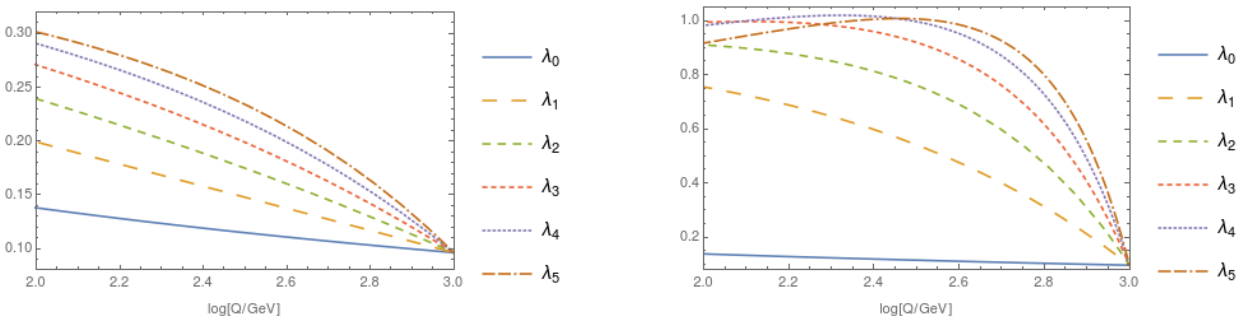

Figure 3.8: RGE running of the Higgs quartic coupling with additional Yukawa couplings of order one and boundary conditions imposed at the TeV scale. The number of additional Yukawa couplings is given by n, $n = 0$ corresponds to the case of the Standard Model. Left, yukawas equal to 1.0, right 2.0

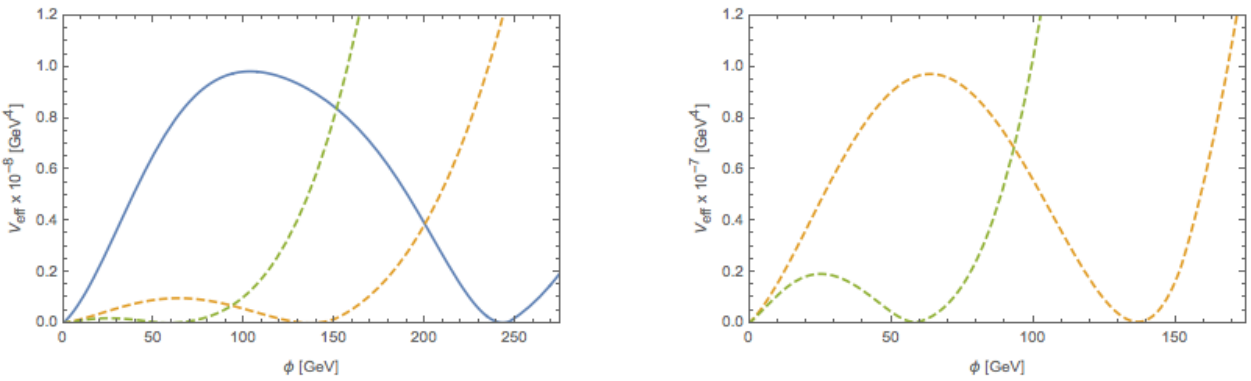

Figure 3.9: The effective potential with varying Yukawa couplings. Solid blue line: The effective potential with $y_1 = 2.0$, and Standard Model values of the Higgs sector parameters. Dashed lines: The effective potential with RGE-improved values of the Higgs sector parameters. The orange curve uses $y_1 = 1.0$; the green curve uses $y_1 = 2.0$.

At the electroweak scale, the parameters of the Higgs potential are $\mu = 89$ and $\lambda = 0.13$. This allows for a first order phase transition with varying Yukawa couplings at 115 GeV, and shown by the solid blue line in Figure 3.9. However, this does not take into account the effects that additional large Yukawa couplings would have on the running of the RGEs and therefore on the values of the Higgs parameters at that scale.

To account for these effects, the RGEs were run downwards from the TeV scale, with a successively increased number of large Yukawa couplings. The potential of the two most extreme cases are shown, where the top Yukawa coupling retains its Standard Model value but the five additional quark Yukawa couplings are set equal to 1.0 and 2.0, corresponding to the orange and green curves in Figure 3.9.

The large Yukawa couplings increase the value of the quartic coupling at the electroweak scale, which in turn lowers both the vev and the temperature at which a phase transition occurs. For a transition to be considered strongly first order, it must meet the condition that ϕ_c/T_c [48]. In the case of the additional five quark Yukawa couplings equal to 1.0, shown by the orange curve in Figure 3.9, the quartic coupling increases to 0.27 which lowers the vev to 137 GeV, leading to a Higgs mass of 95 GeV. In this scenario the critical temperature decreases to 112 GeV, and ϕ_c/T_c decreases to 1.23. In the case of additional Yukawa couplings

equal to 2.0, shown by the green curve in Figure 3.9: the quartic coupling increases to 0.97, the vev decreases to only 58 GeV, the critical temperature decreases to 52 GeV, with $\phi_c/T_c = 1.12$. The predicted Higgs mass in this case is also lowered, to 80 GeV.

Chapter 4

Bubble Nucleation

4.1 Bubble Nucleation in the Case of Varying Yukawa Couplings

It is possible to have a parameter space where a first order phase transition is expected, but bubbles fail to nucleate, as shown in [10]. In this section, we will look at the bubble nucleation dynamics for the case of varying Yukawa couplings using the Python program CosmoTransitions [49]and see that just satisfying $\phi_c/T_c \gtrsim 1.0$ does not capture the full picture.

For instance, one can have two potentials, with similar critical temperatures and similar values of ϕ_c (so that they both satisfy ϕ_c/T_c), but one has a very tall barrier and the other has a more modest barrier. This barrier height will affect whether bubbles are able to nucleate or not.

In the toy model presented above with $y_1 = 2.0$ and all Yukawa couplings set to $y_0 = 0.02$, bubbles fail to nucleate, even though $\phi_c/T_c \gtrsim 1.0$ is true. However, if we refine the model to

include the physical masses of the quarks (as opposed to setting $y_0 = 0.02$ for all), it does appear that bubbles can nucleate for certain values of n and y_1. This is likely due to the fact that the potential barrier is lower in the case with physical masses as seen in Fig. 4.1, allowing the action to reach the required $S/T \approx 140$ threshold.

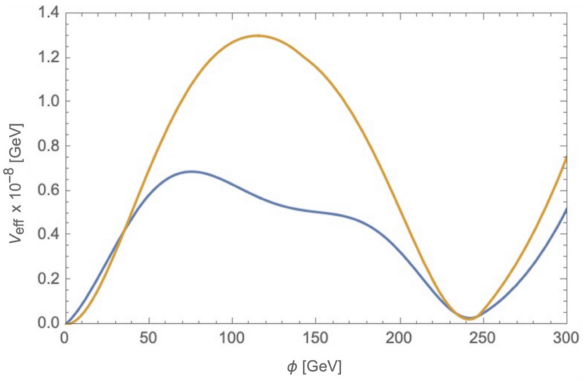

Figure 4.1: The effective potential at the critical temperature. Blue curve: physical Yukawas; Orange curve: all Yukawas set to $y_0 = 0.02$. The tall barrier in the latter case prevents bubbles from nucleating.

In Fig 4.2, we can see there is a region of parameter space where a first order phase transition may be possible if we take bubble nucleation into account, whereas in the toy model with all Yukawa couplings set to 0.02 bubbles do not nucleate anywhere.

However, there are problems with increasing the Yukawa couplings, besides those noted in Section 3. The large Yukawas can lead to questionable forms of the effective potential near the critical temperature due to the large variations in the finite and zero temperature fermion contributions with increasing values of y_1.

As can be seen along the bottom edge of the parameter space, where y_1 is large it would appear that bubbles can nucleate; however the form of the potential is undesirable. Additionally, CosmoTransitions is not reliable for potentials of this form, so a more nuanced approach must be taken to determine if bubbles do in fact nucleate in such a region.

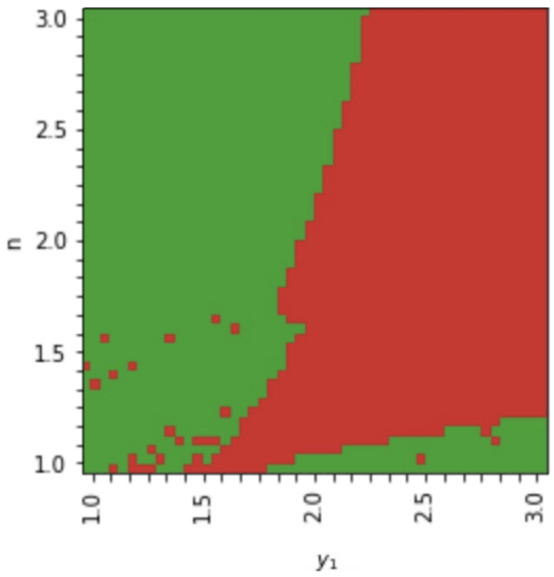

Figure 4.2: Bubble nucleation for various values of n and y_1. Red indicates no phase transition, green indicates first order phase transition.

Along the left edge of parameter space, bubbles are able to nucleate. As can be seen in Fig. 3.5, varying n does not seem to have much effect on the shape of the effective potential. Values greater than one merely cause the Yukawa couplings to decrease at a faster rate, approximating more closely to the Standard Model case where they do not vary at all, so this is expected. Large values of y_1 with $n = 1$, do on the other hand, have a substantial effect.

The large values of y_1 seem to make the barrier too large for bubbles to nucleate, so a smaller y_1 is needed if this mechanism is to be successful. However, a smaller y_1 also has the effect of weakening the phase transition for successful baryogenesis, so a balance must be found.

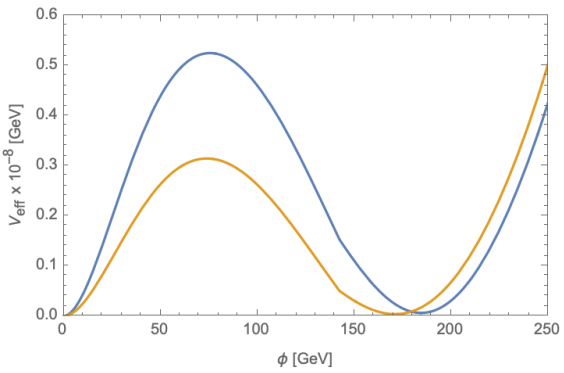

(a) Effective potential at the critical temperature. Blue curve: y_1,$n = 2$, bubbles do not nucleate. Orange curve: $y1 = 1.5$, $n = 2$, bubbles do nucleate, likely due to the lower barrier height.

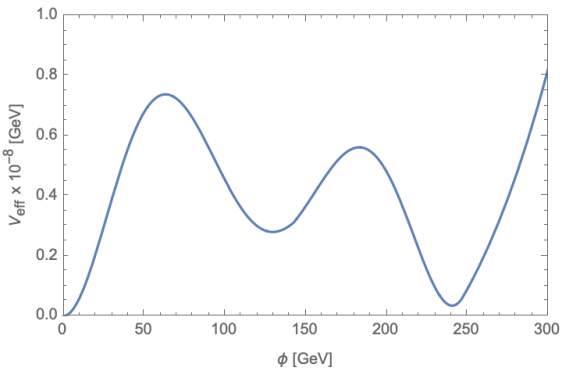

(b) Effective potential for $y1 = 3$, $n = 1$. Bubble nucleation resuls from potentials of this form are not reliable.

Figure 4.3: The full effective potential for different points in parameter space.

4.2 Electroweak Phase Transition with Additional Scalars

In order to vary the Yukawa couplings and implement the Froggatt-Nielsen mechanism, at least one additional scalar field is necessary. If we consider a case with a single additional scalar field, the tree-level potential takes the form

$$V = -\frac{\mu^2}{2}\phi^2 + \frac{\lambda}{4}\phi^4 - \frac{m_0^2}{2}\sigma^2 + \frac{\eta}{4}\sigma^2 + \frac{\kappa}{4}\phi^2\sigma^2. \tag{4.1}$$

The masses squared of the Higgs and flavon are given by the eigenvalues of the scalar mass matrix

$$\begin{bmatrix} m_{\phi\phi}^2 & m_{\sigma\phi}^2 \\ m_{\phi\sigma}^2 & m_{\sigma\sigma}^2 \end{bmatrix}, \tag{4.2}$$

where

$$m^2_{\phi\phi} = \frac{\partial^2 V(\phi,\sigma)}{\partial\phi^2} = -\mu^2 + 3\lambda\phi^2 + \tfrac{1}{2}\kappa\sigma^2 \tag{4.3}$$

$$m^2_{\sigma\sigma} = \frac{\partial^2 V(\phi,\sigma)}{\partial\sigma^2} = -m_0^2 + 3\eta\sigma^2 + \tfrac{1}{2}\kappa\phi^2 \tag{4.4}$$

$$m^2_{\phi\sigma} = \frac{\partial^2 V(\phi,\sigma)}{\partial\phi\partial\sigma} = \kappa\phi\sigma, \tag{4.5}$$

and the eigenvalues in the mass basis are given by

$$m^2_{\phi} = \frac{1}{2}\left(m^2_{\phi\phi} + m^2_{\sigma\sigma} + \sqrt{(m^2_{\phi\phi} - m^2_{\sigma\sigma})^2 + 4m^4_{\phi\sigma}}\right) \tag{4.6}$$

$$m^2_{\sigma} = \frac{1}{2}\left(m^2_{\phi\phi} + m^2_{\sigma\sigma} - \sqrt{(m^2_{\phi\phi} - m^2_{\sigma\sigma})^2 + 4m^4_{\phi\sigma}}\right). \tag{4.7}$$

In a potential with an additional scalar, we are interested in what is called a 2-step phase transition. This means that at high temperatures the potential is in the symmetric phase with the vev at $(0,0)$, as the temperature decreases to a new local minima along the σ axis at $(0, v_\sigma)$. There is a phase transition at this time, and the flavon obtains a vev. As the temperature decreases further, another deeper minimum develops along the ϕ access at $(v_\phi, 0)$, and the electroweak phase transition occurs as the field tunnels from $(0, v_\sigma) \to (v_\phi, 0)$.

Since for this case we want our Higgs and flavon vevs to develop in a specific location and have a specific tree-level potential, the minimum along the ϕ axis will be located at $(\mu/\sqrt{\lambda}, 0)$ and $(0, m_0/\sqrt{\eta})$.

The reason that such a phase transition is desirable is that it allows the Yukawa couplings to change according to the vevs of both scalar fields (the Higgs and the flavon). There are different types of 2-step phase transitions. In some models it is not necessary for the flavon to obtain a value of zero for its final vev, for example, in the model described in [50] a final value equal to $v_\sigma/5$ is desirable.

4.2.1 Bubble Nucleation with Additional Scalar

Here, we will follow the two scalar model with varying yukawas proposed in [9]. We assume the Yukawa couplings are a function of the additional scalar field σ. The fermion masses were taken to be of the form

$$m_i(\phi, \sigma) = y_i \left(\frac{\sigma}{\sqrt{2}\Lambda} \right)^{n_i} \frac{\phi}{\sqrt{2}}, \tag{4.8}$$

where n is determined by the Froggatt-Nielsen charges of each fermion, and y_i is an order one constant chosen such that the mass function returns the correct physical mass of the particle at the vev.

We will consider two-step phase transitions, with the vev pattern of $(0,0) \to (0, v_\sigma) \to (v_\phi, 0)$.

It was pointed out in [10] that in many scenarios with a two-step phase transition for points where a first order phase transitions is naively expected, no phase transition occurs because bubbles fail to nucleate. The main issue is that if a barrier exists down to zero temperature, the action is then bounded from below and never reaches the required $S/T \approx 140$ criterion.

If we look at a cross section of the parameter space studied in [50], we can see that bubbles only nucleate in a small range of parameters where the barrier height is not too tall. In Fig. 4.4, CosmoTransitions is run over the parameter space from $\kappa = 10^{-3.0}$ to $10^{0.0}$ and $\eta = 10^{-3.2}$ to $10^{-4.4}$.

To gain some insight into why only a small region is allowed, we plot in Fig. 4.7 individual effective potentials in the region where bubbles nucleate and in the region where they do not. Bubbles only nucleate in the area roughly corresponding to potentials with no (or extremely small) tree-level barrier between the symmetric and broken phase. This in turn implies a not-too-tall barrier at the critical temperature.

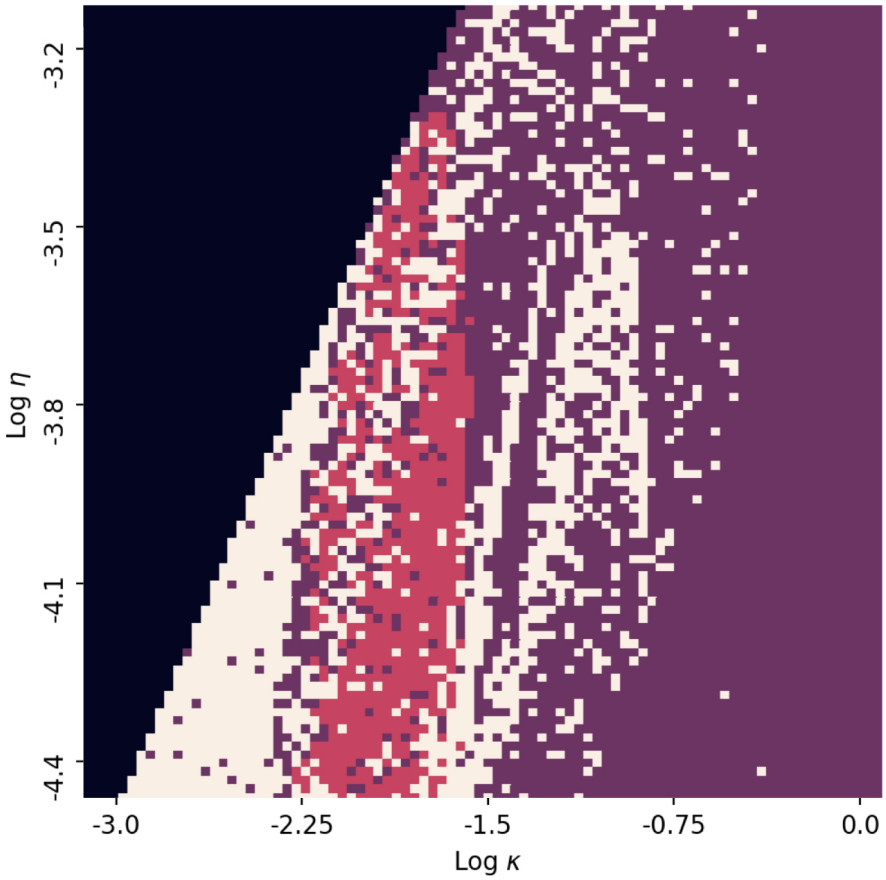

Figure 4.4: Bubble nucleation for case with varying Yukawas and additional scalar. Purple: no phase transition; Pink: first order phase transition; black: non viable vacuum structure, White: bubbles likely do not nucleate, but more precision is needed.

We see that the barrier height at the critical temperature, all the way down to zero temperature, plays a critical role in determining if bubbles nucleate or not. This is seen in Fig. 4.8, where the region corresponding to a first order phase transition is the region with no tree-level barrier. The barriers between the symmetric and broken phase increase in height as we move to the top right of the parameter space, again corresponding to the region where bubbles fail to nucleate.

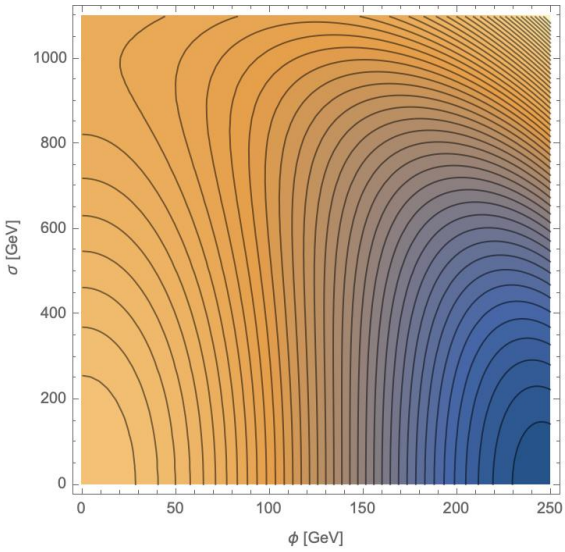

(a) The case with $\eta = 10^{-4}$ and $\kappa = 10^{-2}$. Bubbles do nucleate in this case.

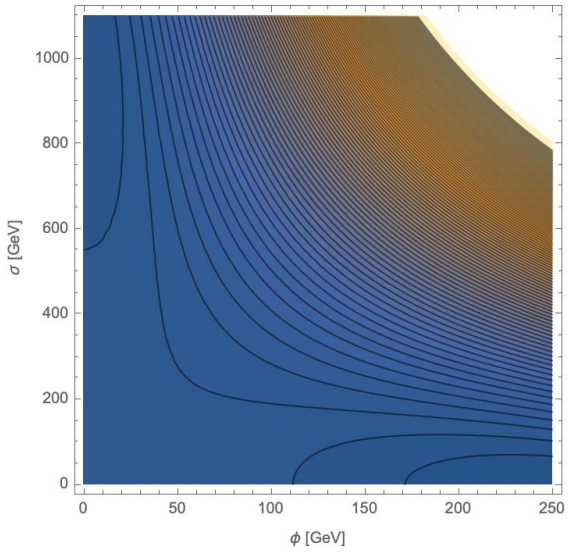

(b) The case with $\eta = 10^{-3.467}$, $\kappa = 10^{-0.333}$. Bubbles do not nucleate in this case.

Figure 4.5: Tree-level potentials.

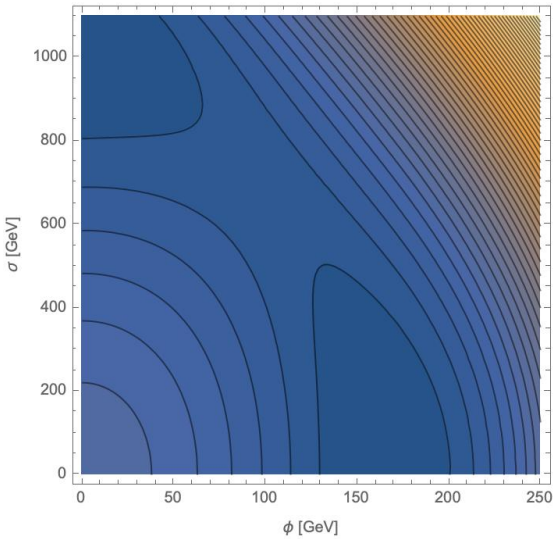

(a) The case with $\eta = 10^{-4}$ and $\kappa = 10^{-2}$. Bubbles do nucleate in this case.

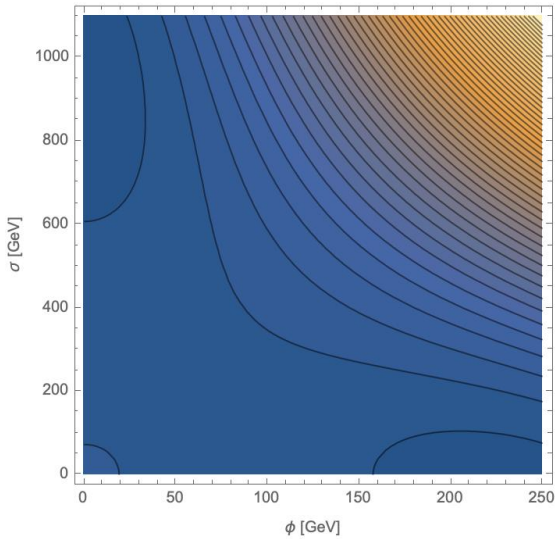

(b) The case with $\eta = 10^{-3.467}$, $\kappa = 10^{-0.333}$. Bubbles do not nucleate in this case.

Figure 4.6: Effective potential at the critical temperature.

4.2.2 Effects of Daisy Correction on Bubble Nucleation

The daisy correction is important for effective potential calculations because it is of order ϕ^3, which contributes to first order phase transitions. However, in our cases it did not have

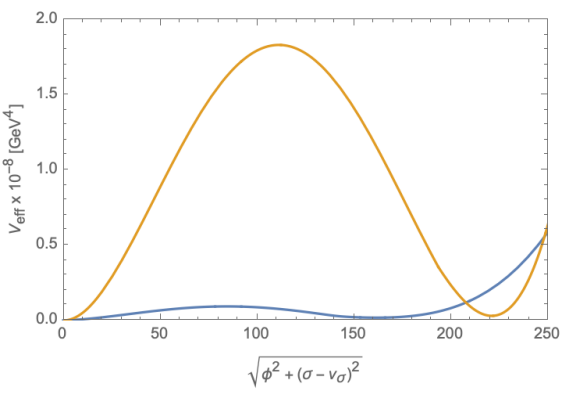

(a) Effective potential at the critical temperature, blue curve nucleates orange does not.

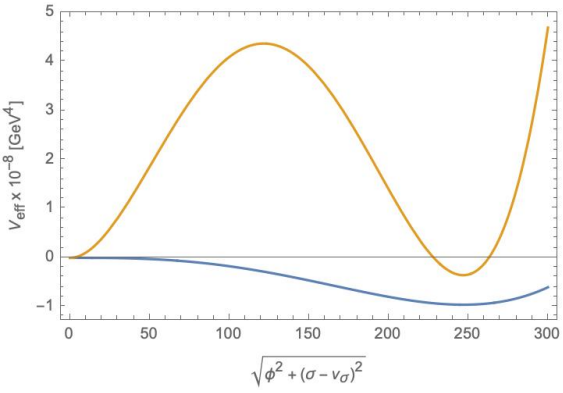

(b) Tree-level potential, blue curve nucleates orange does not.

Figure 4.7: Effective and tree level potentials. Blue curve: $\eta = 10^{-4}$ and $\kappa = 10^{-2}$; Orange curve: $\eta = 10^{-3.467}$, $\kappa = 10^{-0.333}$.

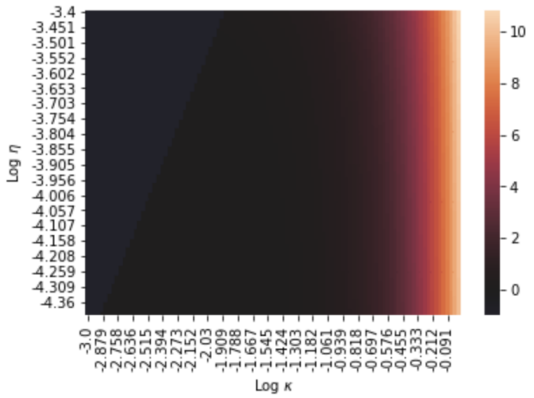

(a) Barrier height at the tree-level.

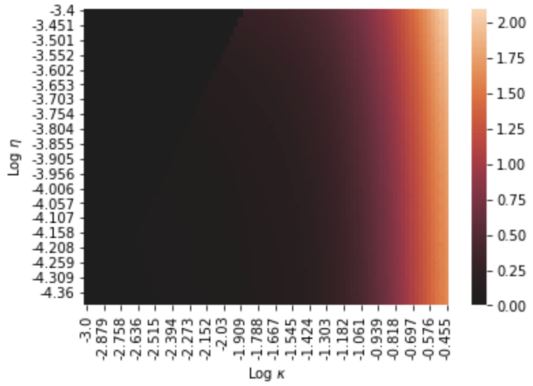

(b) Barrier height at critical temperature.

Figure 4.8: Barrier heights for potentials at their respective critical temperatures and tree-level. In units of GeV^4.

a significant effect whether bubbles nucleated or not.

In the case of the varying Yukawa couplings and no additional scalar described in Section 3, the larger the value of y_1 the more drastic the daisy contribution is changed from the Standard Model case, as can be seen in Fig. 4.9. As mentioned previously, this has the effect of lowering the critical temperature and hence delaying the phase transition, but it has almost no effect on the barrier height as can be seen in Fig. 4.10.

While the daisy contribution is affected most significantly when y_1 is larger, this will not have

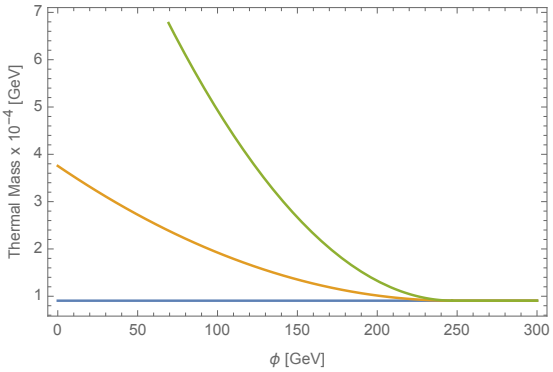

(a) Thermal mass of Higgs.

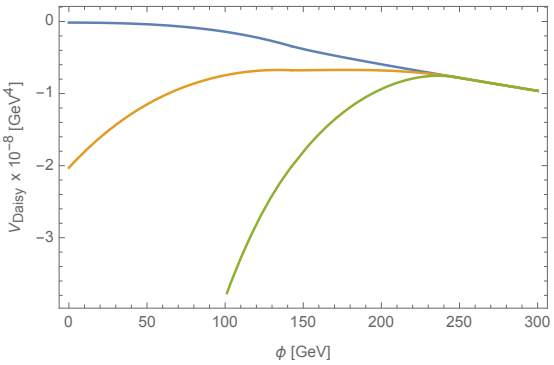

(b) Daisy Contribution of Higgs.

Figure 4.9: Blue: daisy contribution with Standard Model thermal mass; Orange: daisy contribution with varying Yukawas and $y_1 = 1.0$; Green: daisy contribution with varying Yukawas and $y_1 = 2.0$.

a noticeable affect on the nucleation of bubbles because as y_1 gets larger, so does the barrier height. Increasing the barrier height in a region where bubbles already cannot nucleate will only make the situation for bubble nucleation worse.

At smaller values of y_1 the daisy correction has a smaller contribution to the effective potential compared to the Standard Model case, which only slightly raises the barrier at the critical temperature. This is likely to only have an effect on the edge cases where bubbles nucleate or not.

The same is true for the additional scalar case, where the daisy correction does not have a significant effect on bubble nucleation.

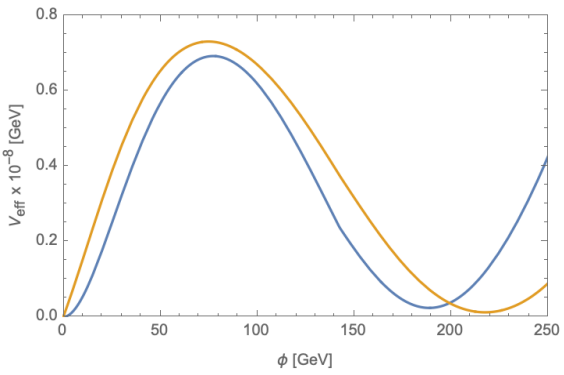

(a) With and without the daisy correction, for $y_1 = 2$, $n = 2$. Bubbles do not nucleate in this case.

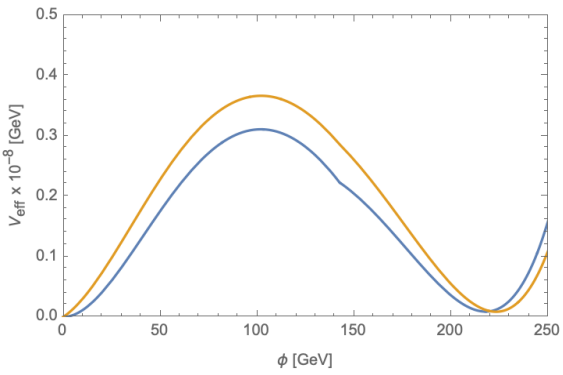

(b) With and without the daisy correction, $y_1 = 1$, $n = 1$. Bubbles can nucleate here.

Figure 4.10: Effective potential at the critical temperature for the case of varying Yukawas with and without the daisy correction. Blue curve: no daisy correction; Orange curve: including daisy correction. The daisy correction has the effect of lowering the critical temperature but does not significantly affect the barrier height in either case.

Chapter 5

Conclusion

Electroweak baryogenesis is an attractive solution to the matter-antimatter asymmetry in our universe due to both its theoretical feasibility and experimental accessibility. The possibility that electroweak baryogenesis is connected to the flavor problem and the cosmological implications of that have not been studied to a large extent. However, in the scenarios studied so far there remain some issues.

Requiring that the electroweak phase transition in the Standard Model be strongly first order constrains the Higgs mass to be $m_H < 72$ GeV. With an observed Higgs mass of 125 GeV, it is clear that a strongly first order electroweak phase transition requires physics beyond the Standard Model. A new scenario was proposed in [51, 50, 9] which introduces the idea that large Yukawa couplings could cause a strongly first order electroweak phase transition.

The Higgs quartic coupling in the Standard Model is positive up to around 10^{10} GeV, where the quartic coupling then turns negative, making the Higgs scalar potential unstable. If additional Yukawa couplings of order one are present before the electroweak phase transition, the Higgs potential will become unstable at a much lower scale. If the large Yukawa couplings are present at the TeV scale, the Higgs quartic coupling is driven to be larger at

the electroweak scale than its Standard Model value. This in turn predicts a lighter Higgs than the measured value.

In addition to the inconsistency with the observed Higgs mass, there also exist severe constraints [52] from cosmology on the proposed scenario with varying Yukawa couplings. All together, these limitations render this simplest setup with large varying Yukawa couplings not a viable mechanism for baryogenesis.

More complex models have been proposed, mainly the addition of extra BSM scalars. But these also have their issues. The main problem is that in much of the parameter space, there remains a rather large barrier separating the symmetric and broken phase, which stops bubbles from nucleating and thus the phase transition cannot proceed.

However, it does seem that there is a quantifiable relationship between the barrier height and the probability of nucleating bubbles, and this will require further investigation. It would be useful to have a method that is both more robust than the simple $\phi_c/T_C \gtrsim 1.0$ criteria, and yet simpler than running cosmotransitions or performing lattice or Monte Carlo simulations.

It would be interesting to possibly apply some machine learning techniques to this, it is possible to examine a large section of parameter space using a program like cosmoTransitions to classify the nature of the phase transition at every point, and compare that information with information on the barrier height, width, critical temperature, or a combination thereof to determine what characteristic has the strongest correlation with each type of phase transition.

This would be very beneficial because it would introduce a new and simpler way to take into account bubble nucleation, by simply calculating certain features of the effective potential instead of running somewhat complicated programs. Since we know that barrier height has a significant effect on bubble nucleation, this would likely be a fruitful avenue of research and a simple application of machine learning.

Other developments in machine learning are also promising, such as in [53] that solves the differential equations and optimization problems associated with cosmological phase transitions. This is a promising new avenue of research as it may allow more accurate solutions to a wide range of problems.

Bibliography

[1] V.A. Kuzmin, V.A. Rubakov, and M.E. Shaposhnikov. On the Anomalous Electroweak Baryon Number Nonconservation in the Early Universe. *Phys. Lett. B*, 155:36, 1985.

[2] David E Morrissey and Michael J Ramsey-Musolf. Electroweak baryogenesis. *New Journal of Physics*, 14(12):125003, Dec 2012.

[3] Vernon Barger, Paul Langacker, Mathew McCaskey, Michael J. Ramsey-Musolf, and Gabe Shaughnessy. LHC Phenomenology of an Extended Standard Model with a Real Scalar Singlet. *Phys. Rev. D*, 77:035005, 2008.

[4] Jose Ramon Espinosa and Mariano Quiros. Novel Effects in Electroweak Breaking from a Hidden Sector. *Phys. Rev.*, D76:076004, 2007.

[5] Jose R. Espinosa, Thomas Konstandin, and Francesco Riva. Strong Electroweak Phase Transitions in the Standard Model with a Singlet. *Nucl. Phys. B*, 854:592–630, 2012.

[6] Laurent Canetti, Marco Drewes, and Mikhail Shaposhnikov. Matter and Antimatter in the Universe. *New J. Phys.*, 14:095012, 2012.

[7] M.B. Gavela, P. Hernandez, J. Orloff, O. Pene, and C. Quimbay. Standard model CP violation and baryon asymmetry. Part 2: Finite temperature. *Nucl. Phys. B*, 430:382–426, 1994.

[8] Micha Berkooz, Yosef Nir, and Tomer Volansky. Baryogenesis from the kobayashi-maskawa phase. *Phys. Rev. Lett.*, 93:051301, Jul 2004.

[9] Iason Baldes, Thomas Konstandin, and Geraldine Servant. A first-order electroweak phase transition from varying Yukawas. *Phys. Lett.*, B786:373–377, 2018.

[10] Gowri Kurup and Maxim Perelstein. Dynamics of Electroweak Phase Transition In Singlet-Scalar Extension of the Standard Model. *Phys. Rev.*, D96(1):015036, 2017.

[11] R.D. Peccei and Helen Quinn. Cp conservation in the presence of pseudoparticles. *Physical Review Letters - PHYS REV LETT*, 38:1440–1443, 06 1977.

[12] S. Hatakeyama, T. Hara, Y. Fukuda, T. Hayakawa, K. Inoue, K. Ishihara, H. Ishino, S. Joukou, T. Kajita, S. Kasuga, Y. Koshio, T. Kumita, K. Matsumoto, M. Nakahata, K. Nakamura, K. Okumura, A. Sakai, M. Shiozawa, J. Suzuki, Y. Suzuki, T. Tomoeda, Y. Totsuka, K. S. Hirata, K. Kihara, Y. Oyama, M. Koshiba, K. Nishijima,

T. Horiuchi, K. Fujita, M. Koga, T. Maruyama, A. Suzuki, M. Mori, T. Suda, A. T. Suzuki, T. Ishizuka, K. Miyano, H. Okazawa, Y. Nagashima, M. Takita, T. Yamaguchi, Y. Hayato, K. Kaneyuki, T. Suzuki, Y. Takeuchi, T. Tanimori, S. Tasaka, E. Ichihara, S. Miyamoto, and K. Nishikawa. Measurement of the flux and zenith-angle distribution of upward through-going muons in kamiokande $ii + iii$. *Phys. Rev. Lett.*, 81:2016–2019, Sep 1998.

[13] G.L. Fogli, E. Lisi, A. Marrone, D. Montanino, A. Palazzo, and A.M. Rotunno. Global analysis of neutrino masses, mixings and phases: entering the era of leptonic CP violation searches. *Phys. Rev. D*, 86:013012, 2012.

[14] Varun Sahni. Dark matter and dark energy. *Lect. Notes Phys.*, 653:141–180, 2004.

[15] Michael Dine and Alexander Kusenko. The Origin of the matter - antimatter asymmetry. *Rev. Mod. Phys.*, 76:1, 2003.

[16] Benjamin Grinstein. TASI-2013 Lectures on Flavor Physics. In *Theoretical Advanced Study Institute in Elementary Particle Physics: Particle Physics: The Higgs Boson and Beyond*, 1 2015.

[17] K. S. Babu. Tasi lectures on flavor physics, 2009.

[18] Yuval Grossman and Philip Tanedo. Just a Taste: Lectures on Flavor Physics. In *Theoretical Advanced Study Institute in Elementary Particle Physics: Anticipating the Next Discoveries in Particle Physics*, pages 109–295, 2018.

[19] Makoto Kobayashi and Toshihide Maskawa. CP Violation in the Renormalizable Theory of Weak Interaction. *Prog. Theor. Phys.*, 49:652–657, 1973.

[20] A. D. Sakharov. Violation of CP Invariance, C asymmetry, and baryon asymmetry of the universe. *Pisma Zh. Eksp. Teor. Fiz.*, 5:32–35, 1967. [Usp. Fiz. Nauk161,no.5,61(1991)].

[21] D.A. Kirzhnits. Weinberg model in the hot universe. *JETP Lett.*, 15:529–531, 1972.

[22] F. Csikor, Z. Fodor, and J. Heitger. Endpoint of the hot electroweak phase transition. *Phys. Rev. Lett.*, 82:21–24, 1999.

[23] J.I. Kapusta and Charles Gale. *Finite-temperature field theory: Principles and applications*. Cambridge Monographs on Mathematical Physics. Cambridge University Press, 2011.

[24] Valery A. Rubakov and Dmitry S. Gorbunov. *Introduction to the Theory of the Early Universe: Hot big bang theory*. World Scientific, Singapore, 2017.

[25] Mark Trodden. Electroweak baryogenesis. *Rev. Mod. Phys.*, 71:1463–1500, 1999.

[26] Wei Su, Anthony G. Williams, and Mengchao Zhang. Strong first order electroweak phase transition in 2HDM confronting future Z & Higgs factories. 11 2020.

[27] M. Laine and K. Rummukainen. The MSSM electroweak phase transition on the lattice. *Nucl. Phys. B*, 535:423–457, 1998.

[28] Christopher Lee. Baryogenesis and EDMs: Constraining CP violation beyond the standard model. *Journal of Physics: Conference Series*, 69:012036, may 2007.

[29] M. Tanabashi, K. Hagiwara, K. Hikasa, K. Nakamura, Y. Sumino, F. Takahashi, J. Tanaka, K. Agashe, G. Aielli, C. Amsler, M. Antonelli, D. M. Asner, H. Baer, Sw. Banerjee, R. M. Barnett, T. Basaglia, C. W. Bauer, J. J. Beatty, V. I. Belousov, J. Beringer, S. Bethke, A. Bettini, H. Bichsel, O. Biebel, K. M. Black, E. Blucher, O. Buchmuller, V. Burkert, M. A. Bychkov, R. N. Cahn, M. Carena, A. Ceccucci, A. Cerri, D. Chakraborty, M.-C. Chen, R. S. Chivukula, G. Cowan, O. Dahl, G. D'Ambrosio, T. Damour, D. de Florian, A. de Gouvêa, T. DeGrand, P. de Jong, G. Dissertori, B. A. Dobrescu, M. D'Onofrio, M. Doser, M. Drees, H. K. Dreiner, D. A. Dwyer, P. Eerola, S. Eidelman, J. Ellis, J. Erler, V. V. Ezhela, W. Fetscher, B. D. Fields, R. Firestone, B. Foster, A. Freitas, H. Gallagher, L. Garren, H.-J. Gerber, G. Gerbier, T. Gershon, Y. Gershtein, T. Gherghetta, A. A. Godizov, M. Goodman, C. Grab, A. V. Gritsan, C. Grojean, D. E. Groom, M. Grünewald, A. Gurtu, T. Gutsche, H. E. Haber, C. Hanhart, S. Hashimoto, Y. Hayato, K. G. Hayes, A. Hebecker, S. Heinemeyer, B. Heltsley, J. J. Hernández-Rey, J. Hisano, A. Höcker, J. Holder, A. Holtkamp, T. Hyodo, K. D. Irwin, K. F. Johnson, M. Kado, M. Karliner, U. F. Katz, S. R. Klein, E. Klempt, R. V. Kowalewski, F. Krauss, M. Kreps, B. Krusche, Yu. V. Kuyanov, Y. Kwon, O. Lahav, J. Laiho, J. Lesgourgues, A. Liddle, Z. Ligeti, C.-J. Lin, C. Lippmann, T. M. Liss, L. Littenberg, K. S. Lugovsky, S. B. Lugovsky, A. Lusiani, Y. Makida, F. Maltoni, T. Mannel, A. V. Manohar, W. J. Marciano, A. D. Martin, A. Masoni, J. Matthews, U.-G. Meißner, D. Milstead, R. E. Mitchell, K. Mönig, P. Molaro, F. Moortgat, M. Moskovic, H. Murayama, M. Narain, P. Nason, S. Navas, M. Neubert, P. Nevski, Y. Nir, K. A. Olive, S. Pagan Griso, J. Parsons, C. Patrignani, J. A. Peacock, M. Pennington, S. T. Petcov, V. A. Petrov, E. Pianori, A. Piepke, A. Pomarol, A. Quadt, J. Rademacker, G. Raffelt, B. N. Ratcliff, P. Richardson, A. Ringwald, S. Roesler, S. Rolli, A. Romaniouk, L. J. Rosenberg, J. L. Rosner, G. Rybka, R. A. Ryutin, C. T. Sachrajda, Y. Sakai, G. P. Salam, S. Sarkar, F. Sauli, O. Schneider, K. Scholberg, A. J. Schwartz, D. Scott, V. Sharma, S. R. Sharpe, T. Shutt, M. Silari, T. Sjöstrand, P. Skands, T. Skwarnicki, J. G. Smith, G. F. Smoot, S. Spanier, H. Spieler, C. Spiering, A. Stahl, S. L. Stone, T. Sumiyoshi, M. J. Syphers, K. Terashi, J. Terning, U. Thoma, R. S. Thorne, L. Tiator, M. Titov, N. P. Tkachenko, N. A. Törnqvist, D. R. Tovey, G. Valencia, R. Van de Water, N. Varelas, G. Venanzoni, L. Verde, M. G. Vincter, P. Vogel, A. Vogt, S. P. Wakely, W. Walkowiak, C. W. Walter, D. Wands, D. R. Ward, M. O. Wascko, G. Weiglein, D. H. Weinberg, E. J. Weinberg, M. White, L. R. Wiencke, S. Willocq, C. G. Wohl, J. Womersley, C. L. Woody, R. L. Workman, W.-M. Yao, G. P. Zeller, O. V. Zenin, R.-Y. Zhu, S.-L. Zhu, F. Zimmermann, P. A. Zyla, J. Anderson, L. Fuller, V. S. Lugovsky, and P. Schaffner. Review of particle physics. *Phys. Rev. D*, 98:030001, Aug 2018.

[30] Leonardo Leitao, Ariel Megevand, and Alejandro D. Sanchez. Gravitational waves from the electroweak phase transition. *JCAP*, 10:024, 2012.

[31] Amine Ahriche, Katsuya Hashino, Shinya Kanemura, and Salah Nasri. Gravitational waves from phase transitions in models with charged singlets. *Physics Letters B*, 789:119 – 126, 2019.

[32] Sidney R. Coleman and Erick J. Weinberg. Radiative Corrections as the Origin of Spontaneous Symmetry Breaking. *Phys. Rev.*, D7:1888–1910, 1973.

[33] R. Jackiw. Functional evaluation of the effective potential. *Phys. Rev.*, D9:1686, 1974.

[34] Mariano Quiros. Finite temperature field theory and phase transitions. In *Proceedings, Summer School in High-energy physics and cosmology: Trieste, Italy, June 29-July 17, 1998*, pages 187–259, 1999.

[35] Steven Weinberg. Gauge and Global Symmetries at High Temperature. *Phys. Rev. D*, 9:3357–3378, 1974.

[36] Andrey Katz and Maxim Perelstein. Higgs Couplings and Electroweak Phase Transition. *JHEP*, 07:108, 2014.

[37] Sidney R. Coleman. The Fate of the False Vacuum. 1. Semiclassical Theory. *Phys. Rev. D*, 15:2929–2936, 1977. [Erratum: Phys.Rev.D 16, 1248 (1977)].

[38] Greg W. Anderson and Lawrence J. Hall. Electroweak phase transition and baryogenesis. *Phys. Rev. D*, 45:2685–2698, Apr 1992.

[39] Thomas Konstandin and Stephan J. Huber. Numerical approach to multi dimensional phase transitions. *JCAP*, 06:021, 2006.

[40] Michael Dine, Robert G. Leigh, Patrick Y. Huet, Andrei D. Linde, and Dmitri A. Linde. Towards the theory of the electroweak phase transition. *Phys. Rev. D*, 46:550–571, 1992.

[41] Frans R. Klinkhamer and N.S. Manton. A Saddle Point Solution in the Weinberg-Salam Theory. *Phys. Rev. D*, 30:2212, 1984.

[42] Peter Brockway Arnold and Larry D. McLerran. Sphalerons, Small Fluctuations and Baryon Number Violation in Electroweak Theory. *Phys. Rev. D*, 36:581, 1987.

[43] Burkhard Kleihaus, Jutta Kunz, and Yves Brihaye. The Electroweak sphaleron at physical mixing angle. *Phys. Lett. B*, 273:100–104, 1991.

[44] Yves Brihaye and Jutta Kunz. Electroweak bubbles and sphalerons. *Phys. Rev. D*, 48:3884–3890, Oct 1993.

[45] C. D. Froggatt and Holger Bech Nielsen. Hierarchy of Quark Masses, Cabibbo Angles and CP Violation. *Nucl. Phys.*, B147:277–298, 1979.

[46] Arianna Braconi, Mu-Chun Chen, and Geoffrey Gaswint. Revisiting electroweak phase transition with varying yukawa coupling constants. *Physical Review D*, 100(1), Jul 2019.

[47] Florian Staub. Exploring new models in all detail with SARAH. *Adv. High Energy Phys.*, 2015:840780, 2015.

[48] Amine Ahriche. What is the criterion for a strong first order electroweak phase transition in singlet models? *Phys. Rev.*, D75:083522, 2007.

[49] Carroll L. Wainwright. CosmoTransitions: Computing Cosmological Phase Transition Temperatures and Bubble Profiles with Multiple Fields. *Comput. Phys. Commun.*, 183:2006–2013, 2012.

[50] Iason Baldes, Thomas Konstandin, and Geraldine Servant. Flavor Cosmology: Dynamical Yukawas in the Froggatt-Nielsen Mechanism. *JHEP*, 12:073, 2016.

[51] Micha Berkooz, Yosef Nir, and Tomer Volansky. Baryogenesis from the Kobayashi-Maskawa phase. *Phys. Rev. Lett.*, 93:051301, 2004.

[52] Benjamin Lillard, Michael Ratz, M. P. Tait, Tim, and Sebastian Trojanowski. The Flavor of Cosmology. *JCAP*, 1807(07):056, 2018.

[53] Maria Laura Piscopo, Michael Spannowsky, and Philip Waite. Solving differential equations with neural networks: Applications to the calculation of cosmological phase transitions. *Phys. Rev. D*, 100(1):016002, 2019.

[54] H. Arason, D. J. Castano, B. Keszthelyi, S. Mikaelian, E. J. Piard, Pierre Ramond, and B. D. Wright. Renormalization group study of the standard model and its extensions. 1. The Standard model. *Phys. Rev.*, D46:3945–3965, 1992.

[55] M. E. Carrington. The Effective potential at finite temperature in the Standard Model. *Phys. Rev.*, D45:2933–2944, 1992.

Appendix A

Renormalization Group Equations

Appendix A shows the renormalization group equations (RGEs) at one loop that are used in our analysis. The RGEs for the Higgs quartic coupling, and scalar mass at one loop for the Standard Model [54] are

$$\frac{d\lambda}{dt} = \frac{1}{16\pi^2}\beta_\lambda^{(1)}\,, \tag{A.1}$$

$$\frac{d\mu}{dt} = \frac{1}{16\pi^2}\beta_\mu^{(1)}\,, \tag{A.2}$$

where $t = \ln E$, where E is the running scale. The beta-function coefficients are given by

$$\begin{aligned}\beta_\lambda^{(1)} &= 24\lambda^2 - \frac{9}{5}g_1^2\lambda - 9g_2^2\lambda + \frac{9}{8}\left(\frac{3}{25}g_1^4 + \frac{2}{5}g_1^2g_2^2 + g_2^4\right) \\ &\quad +4\lambda\mathrm{Tr}\left(3Y_u^\dagger Y_u + 3Y_d^\dagger Y_d + Y_e^\dagger Y_e\right) \\ &\quad -2\mathrm{Tr}\left(3(Y_u^\dagger Y_u)^2 + 3(Y_d^\dagger Y_d)^2 + (Y_e^\dagger Y_e)^2\right) , \end{aligned} \tag{A.3}$$

$$\begin{aligned}\beta_\mu^{(1)} &= 12\mu\lambda + 2\mu\mathrm{Tr}\left(Y_eY_e^\dagger\right) + 6\mu\mathrm{Tr}\left(Y_dY_d^\dagger\right) + 6\mu\mathrm{Tr}\left(Y_uY_u^\dagger\right) \\ &\quad -\frac{9}{10}g_1^2\mu - \frac{9}{2}g_2^2\mu \, . \end{aligned} \tag{A.4}$$

The gauge couplings for the Standard Model at the one loop level are

$$\frac{dg_i}{dt} = \frac{1}{16\pi^2}\beta_{g_i}^{(1)} \, , \tag{A.5}$$

where the three β_{g_i} functions are expressed as

$$\beta_{g_1}^{(1)} = \frac{41}{10}g_1^3 \, , \tag{A.6}$$

$$\beta_{g_2}^{(1)} = -\frac{19}{6}g_2^3 \, , \tag{A.7}$$

$$\beta_{g_3}^{(1)} = -7g_3^3 \, . \tag{A.8}$$

The RGE's for the Yukawa couplings in the Standard Model at one loop are summarized as

$$\beta_{Y_u}^{(1)} = -\frac{3}{2}\Big(- Y_u Y_u^\dagger Y_u + Y_u Y_d^\dagger Y_d\Big) + Y_u\Big(3\mathrm{Tr}\Big(Y_d Y_d^\dagger\Big) + 3\mathrm{Tr}\Big(Y_u Y_u^\dagger\Big) \tag{A.9}$$
$$-8g_3^2 - \frac{17}{20}g_1^2 - \frac{9}{4}g_2^2 + \mathrm{Tr}\Big(Y_e Y_e^\dagger\Big)\Big)\ ,$$
$$\beta_{Y_d}^{(1)} = \frac{1}{4}\Big(6\Big(- Y_d Y_u^\dagger Y_u + Y_d Y_d^\dagger Y_d\Big) - Y_d\Big(- 12\mathrm{Tr}\Big(Y_d Y_d^\dagger\Big) \tag{A.10}$$
$$-12\mathrm{Tr}\Big(Y_u Y_u^\dagger\Big) + 32g_3^2 - 4\mathrm{Tr}\Big(Y_e Y_e^\dagger\Big) + 9g_2^2 + g_1^2\Big)\Big)\ ,$$
$$\beta_{Y_e}^{(1)} = \frac{3}{2}Y_e Y_e^\dagger Y_e + Y_e\Big(3\mathrm{Tr}\Big(Y_d Y_d^\dagger\Big) + 3\mathrm{Tr}\Big(Y_u Y_u^\dagger\Big) - \frac{9}{4}g_1^2 - \frac{9}{4}g_2^2 \tag{A.11}$$
$$+\mathrm{Tr}\Big(Y_e Y_e^\dagger\Big)\Big)\ .$$

Appendix B

Details of Effective Potential Calculation

B.1 Zero Temperature 1-Loop Correction

To calculate the zero temperature 1-loop correction to the effective potential, one first starts with the zero-loop potential, which in this case is simply the classical (tree-level) potential for a single scalar field as given before

$$V_0(\phi) = \frac{1}{2}m^2\phi^2 + \frac{\lambda}{4}\phi^4, \tag{B.1}$$

with the corresponding lagrangian given by

$$\mathcal{L} = \frac{1}{2}\partial^\mu\phi\partial_\mu\phi - V_0(\phi). \tag{B.2}$$

The zero temperature one-loop correction to this potential is the sum of all of the one particle irreducible (1PI) diagrams with one loop and zero external momenta as described

in Section 2.1.

According to the zero temperature Feynman rules, the n-th 1PI diagram will have n propagators, n vertices, and $2n$ external legs. Each propagator will contribute a factor of $i/(p^2 - m^2 + i\epsilon)$, resulting in an overall contribution of

$$\frac{i^n}{(p^2 - m^2 + i\epsilon)^n}\,. \tag{B.3}$$

The external legs contribute ϕ^{2n} and each vertex contributes $-i\lambda/2$, where the factor of $1/2$ is due to the symmetry of switching the two legs at the vertex. There is an additional overall factor of $1/2n$ from the symmetry of the diagrams under Z_2 and reflection symmetries, as well as one more overall factor of i from the generating functional.

Integrating over the loop-momenta, the contribution has the form

$$V_1 = i\sum_{n=1}^{\infty}\int \frac{d^4p}{(2\pi)^4}\frac{1}{2n}\left(\frac{-i\lambda}{2}\right)^n(\phi_c)^{2n}\frac{i^n}{(p^2 - m^2 + i\epsilon)^n} \tag{B.4}$$

$$= i\sum_{n=1}^{\infty}\int \frac{d^4p}{(2\pi)^4}\frac{1}{2n}\left(\frac{\lambda\phi_c^2}{2(p^2 - m^2 + i\epsilon)}\right)^n. \tag{B.5}$$

We can then use the Taylor series for $\ln(1+x)$ to rewrite the integrand as

$$V_1 = \frac{-i}{2}\int \frac{d^4p}{(2\pi)^4}\ln\left[1 - \frac{\lambda\phi_c^2}{2(p^2 - m^2 + i\epsilon)}\right]. \tag{B.6}$$

Next we perform a Wick rotation and where $p_0 \to ip_E^0$, and $p^2 \to -p_E^2$ to obtain

$$V_1 = \frac{1}{2}\int \frac{d^4p}{(2\pi)^4} \ln\left[1 + \frac{\lambda\phi_c^2}{2(p_E^2 + m^2)}\right]. \tag{B.7}$$

We then use the shifted mass $m_c^2 = m^2 + \frac{1}{2}\lambda\phi_c^2$ to rewrite the log term, ignoring terms not dependent on ϕ, to obtain

$$V_1 = \frac{1}{2}\int \frac{d^4p}{(2\pi)^4} \ln[p^2 + m_c^2], \tag{B.8}$$

which then needs to be renormalized. The renormalized form will then be the zero temperature one-loop correction given in Section 2.1

B.2 Finite Temperature 1-Loop Correction

To calculate the one loop finite-temperature contribution, we follow the same procedure as the one loop zero-temperature contribution, but the finite-temperature Feynman rules are used instead. The finite-temperature Feynman rules have the following form:

Boson propagator: $$\frac{i}{p^2 - m^2} \quad \text{where} \quad p^\mu = \left[\tfrac{2\pi n i}{\beta}, \vec{p}\right] \tag{B.9}$$

Loop integral: $$\frac{i}{\beta} \sum_{n=-\infty}^{\infty} \int \frac{d^3p}{(2\pi)^3} \tag{B.10}$$

Vertex: $$-i\beta(2\pi)^3 \delta_{\sum \omega_i} \delta^3 \left(\sum_i \vec{p}_i \right). \tag{B.11}$$

Following a similar procedure as for the zero-temperature contribution by summing over all 1PI diagrams, we obtain

$$V_1^\beta = \frac{1}{2\beta} \sum_{n=-\infty}^{\infty} \int \frac{d^3p}{(2\pi)^3} \ln \left[1 - \frac{\lambda \phi_c^2/2}{p^2 - m^2} \right]. \tag{B.12}$$

We then again perform a Wick rotation, taking $p^2 \to -p_E^2$, and again replacing the mass with the shifted mass. Considering only the log term, this yields

$$\begin{aligned} \ln[p^2 + m_c^2] &= \ln \left[\left(\frac{2\pi n}{\beta} \right)^n + \vec{p}^2 + m_c^2 \right] \\ &= \ln[\omega_n^2 + \omega^2], \end{aligned} \tag{B.13}$$

where ω_n are the bosonic Matsubara frequencies. (The zero modes of these Matsubara frequencies, where $n = 0$ are the source of our later problems leading to the Daisy correction.)

Summing over the Matsubara frequencies yields

$$V_1^{\beta} = \int \frac{d^3p}{(2\pi)^3} \left[\frac{\omega}{2} + \frac{1}{\beta} \ln \left(1 - e^{-\beta\omega} \right) \right], \tag{B.14}$$

where the first term in the brackets corresponds to the 1-loop zero temperature contribution we obtained previously. Assuming spherical symmetry and replacing ω with $\sqrt{p^2 + m^2}$ we are now left with

$$\frac{1}{2\pi^2\beta} \int dp\; p^2 \ln \left(1 - e^{-\beta\sqrt{p^2+m^2}} \right). \tag{B.15}$$

Making a final substitution of $x \to \beta\, p$ and $dx \to \beta\, dp$ we obtain

$$\frac{1}{2\pi^2\beta^4} \int_0^{\infty} dx\, x^2 \ln \left[1 - e^{-\sqrt{x^2+\beta^2 m^2}} \right]. \tag{B.16}$$

The integral here represents the thermal bosonic function, $J_B[m^2\beta^2]$ as given in eq. 2.11.

Appendix C

The Daisy Correction

As mentioned in Section 2.1, the Daisy contribution is important because it is of order ϕ^3, which is the term in the effective potential that can give rise to a first order phase transition. Infrared divergences in the Matsubara zero modes (when $n = 0$) must be summed over to obtain the correct contribution. Starting with the form for the full finite temperature correction as given in [55]

$$V = -\frac{T}{2} \sum_{n=-\infty}^{\infty} \int \frac{d^3p}{(2\pi)^3} \sum_{N=1}^{\infty} \frac{1}{N} \left(\omega_n^2 + \vec{p}^2 + m^2)\Pi\right)^N , \tag{C.1}$$

where Π is the thermal mass of the boson calculated from the two-point function. We rewrite the second sum as a natural log, which then becomes

$$\frac{T}{2} \sum \int \frac{d^3p}{(2\pi)^3} \ln \left[1 + \frac{\Pi}{\omega_n^2 + p^2 + m^2}\right], \tag{C.2}$$

where m is again the shifted mass $m^2 \to m^2 + \frac{1}{2}\phi^2$.

Re-writting the log term, we see that we obtain

$$\log\left(\omega_n^2 + p^2 + m^2 + \Pi\right) - \ln\left(\omega_n^2 + p^2 + m^2\right). \tag{C.3}$$

Here we can see that the second term is actually the same as the 1-loop contribution, so we have recovered the 1-loop contribution while calculating the daisy contribution.

From the one-loop calculation we know that

$$\frac{T}{2}\sum\int \frac{d^3p}{(2\pi)^3}\ln\left(\omega_n^2 + p^2 + m^2\right) = \frac{1}{2\pi^2\beta^4}J_B(m^2\beta^2)\,, \tag{C.4}$$

and we can rewrite the right hand side as

$$\frac{1}{2\pi^2\beta^4}\left(J_B((m^2+\Pi)\beta^2) - J_B(m^2\beta^2)\right). \tag{C.5}$$

Substituting in the high temperature approximations for the thermal bosonic function we obtain finally

$$V_{\text{Daisy}} = -\frac{T}{12\pi}\left((m^2(\phi) + \Pi(T))^{3/2} - m^3(\phi)\right)\,,$$

which is our daisy contribution.